Direct Aerosol Forcing Effects:
Evaluations from the AEROCLOUDS Measurements in the Po Valley (Northern Italy)

C. Tomasi, C. Lanconelli, A. Lupi and M. Mazzola

Institute of Atmospheric Sciences and Climate (ISAC),
National Council of Research (CNR),
CNR Research Campus,
Via Gobetti 101, Bologna, Italy

Workshop on "Remote sensing of atmospheric aerosol, clouds, and aerosol-cloud interactions", Bremen, December 16 – 19, 2013

CONTENTS

Aerosol radiative properties can vary greatly from one region to another, as a function of their origin and transport features. Thus, the radiative effects caused by aerosols on the radiation budget of the surface-atmosphere system are studied in general over regional scales.

In the present calculations, we have used the following measurements:
(i) local ground-based measurements performed with sun/sky-radio-meters, sun-photometers, and lidar systems,
(ii) level 3.0 MODIS surface reflectance products, and
(iii) *in-situ* particulate matter samplings, used to compare the particle chemical composition and radiative data of fine and coarse aerosol particle fractions with those derived from sun-photometer measure-ments.

These measurements have been used to (1) calculate the variations in the downwelling and upwelling fluxes of solar radiation due to columnar aerosol particles, and (2) evaluate the corresponding direct radiative forcing (DARF) terms induced by columnar aerosol at the ToA- and BoA-levels, and in the Atmosphere.

Direct aerosol-induced radiative forcing (DARF) effects have been evaluated by us on the basis of the aerosol data collected during the following regional experiments:

- **CLEARCOLUMN (ACE-2) experiment in Southern Portugal (summer 1997).**
- **PRIN-2004 experiment conducted at Lecce (Puglia, Southern Italy) in 2003/2004.**
- **AEROCLOUDS experiment conducted at San Pietro Capofiume (Po Valley, Northern Italy) from May 2007 to March 2008.**
- **Ev-K2-CNR campaigns performed in summer 1991 and summer 1992 at the CNR Pyramid Laboratory (Mt. Everest, Himalaya).**
- **POLAR-AOD field measurements performed at Arctic and Antarctic sites during the International Polar Year.**
- **Aerosols99 cruise across the Atlantic Ocean in January 1999.**
- **DOE/ARM/AIOP project conducted in North-central Oklahoma (USA) in May 2003.**

We present here the analysis of field data and DARF evaluations derived from the measurements carried out during the AEROCLOUDS experiment performed in 2007 and 2008.

DEFINITIONS

(A) The instantaneous DARF term $\Delta F(t)_{ToA}$ induced by the columnar aerosol particles at the Top-of-Atmosphere (ToA) level and at a certain time *t* of the day by the columnar aerosol particles can be represented for clear-sky conditions in terms of the following difference:

$$\Delta F(t)_{ToA} = F(t)_{net} - F(t)_{net}^{*} = F\uparrow_{ToA}(t)^{*} - F\uparrow_{ToA}(t) \quad , \qquad (1)$$

between (a) the short-wave upwelling flux $F\uparrow(t)^{*}$ calculated at the ToA-level in a pristine atmosphere without aerosols, and (b) the short-wave upwelling flux $F\uparrow(t)$ determined at the ToA-level in the atmosphere with aerosols.

(B) The instantaneous DARF term $\Delta F(t)_{BoA}$ induced at the Bottom-of-Atmosphere (BoA) level and at a certain time *t* gives a measure of the change induced by columnar aerosol in the net flux of short-wave radiation reaching the surface. Therefore, it can be defined as the difference

$$\Delta F(t)_{BoA} = \Phi(t)_{net} - \Phi(t)_{net}^{*} \quad , \qquad (2)$$

between the net flux $\Phi(t)_{net}$ at the surface determined in the atmosphere with aerosols, and the net flux $\Phi(t)_{net}^{*}$ calculated in the pristine atmosphere without aerosols.

The calculations of the two instantaneous terms $\Delta F(t)_{ToA}$ and $\Delta F(t)_{BoA}$ **(both consisting of direct and diffuse short-wave radiation components)** have been made using a procedure, based on the 6S (Second Simulation of the Satellite Signal in the Solar Spectrum) radiative tranfer code for:

(a) realistic representations of the atmosphere, made for the vertical profiles of temperature, pressure, and moisture parameters derived from local meteorological radiosounding measurements,

(b) field measurements of aerosol optical thickness $\tau_a(\lambda)$ at various visible and near-infrared wavelengths, and

(c) columnar aerosol radiative properties (i.e., complex refractive index, phase function, asymmetry factor, single scattering albedo) obtained by retrieving the sun-photometer measurements of sky-brightness in the almucantar.

The instantaneous DARF terms $\Delta F(t)_{ToA}$ and $\Delta F(t)_{BoA}$ **were calculated to evidence the dependence features on**

solar zenith angle θ_o during the sunlit period,
columnar aerosol radiative parameters,
aerosol optical thickness $\tau_a(\lambda)$, and
surface reflectance characteristics.

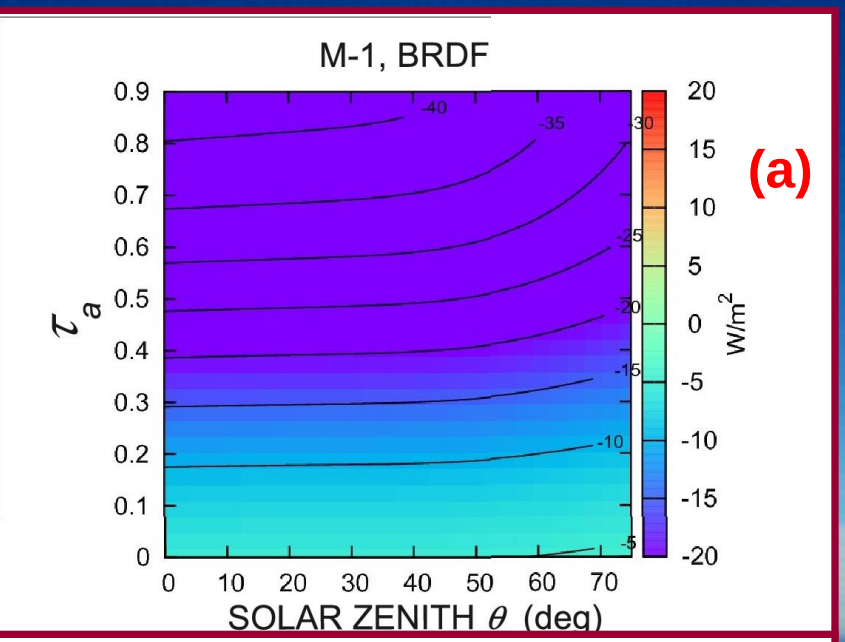

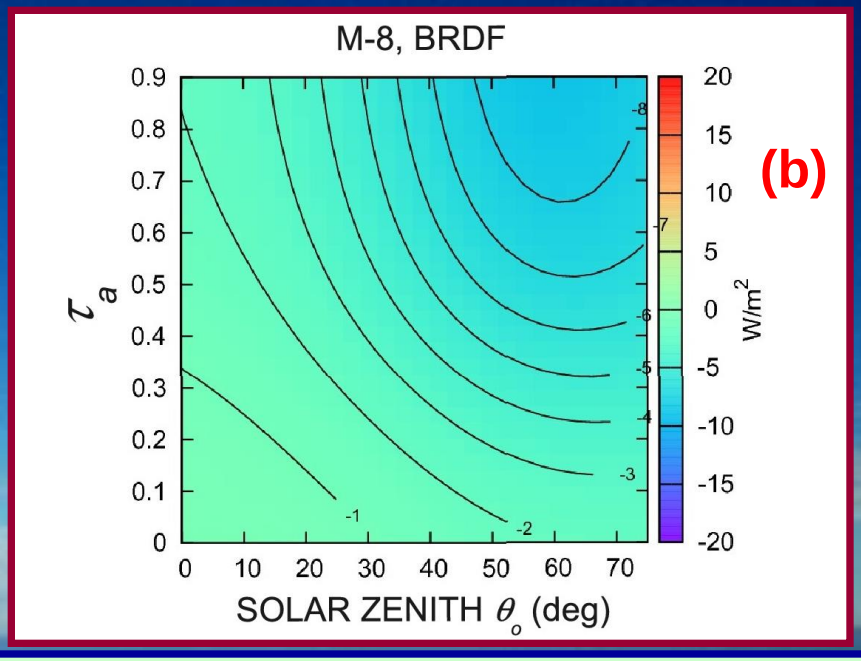

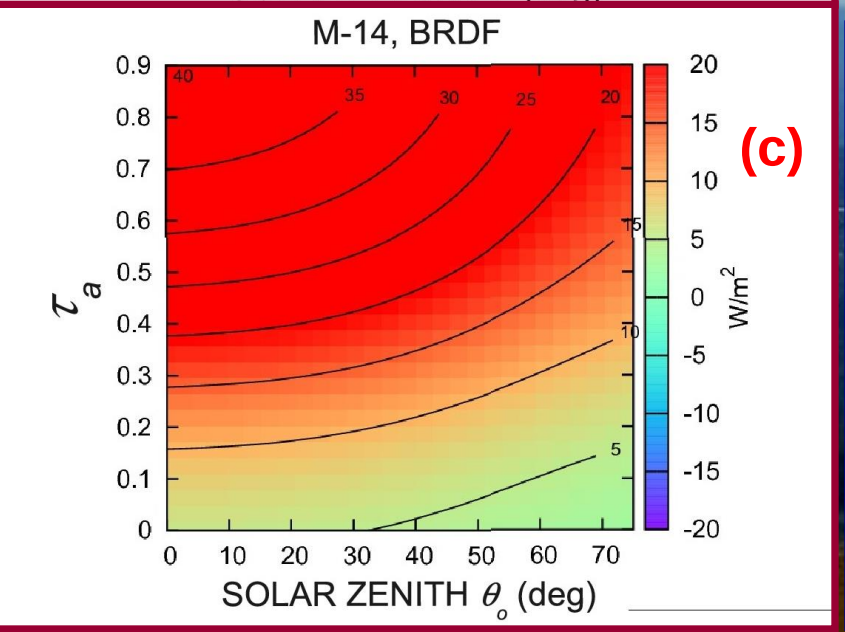

Mesh plots of the short-wave instantaneous DARF term $\Delta F(t)_{ToA}$ as a function of aerosol optical thickness $\tau_a(0.55\ \mu m)$ (in ordinate) and solar zenith angle θ_o (in abscissa) for three aerosol cases (a) pure maritime aerosol model M-1; (b) pure continental aerosol model M-8; and (c) heavy polluted aerosol model M-14, all suspended over a vegetation-covered surface represented by the non - Lambertian reflectance model VS3.

Instantaneous DARF terms ΔF_{ToA} (upper part) and ΔF_{BoA} (lower part) plotted versus the weighted average columnar aerosol single scattering albedo ω^* (ranging between 0.6 and 1.0) for the 14 M-type aerosol models, all giving $\tau_a(0.55\ \mu m)$ = 0.30, and for solar zenith angles θ_o = 30° (left) and θ_o = 60° (right), as calculated over the OS1 (blue), VS2 (green), BS3 (red) and PS1 (gray) non-Lambertian surface reflectance models (light colours) and equivalent isotropic surface reflectance models (darker colours).

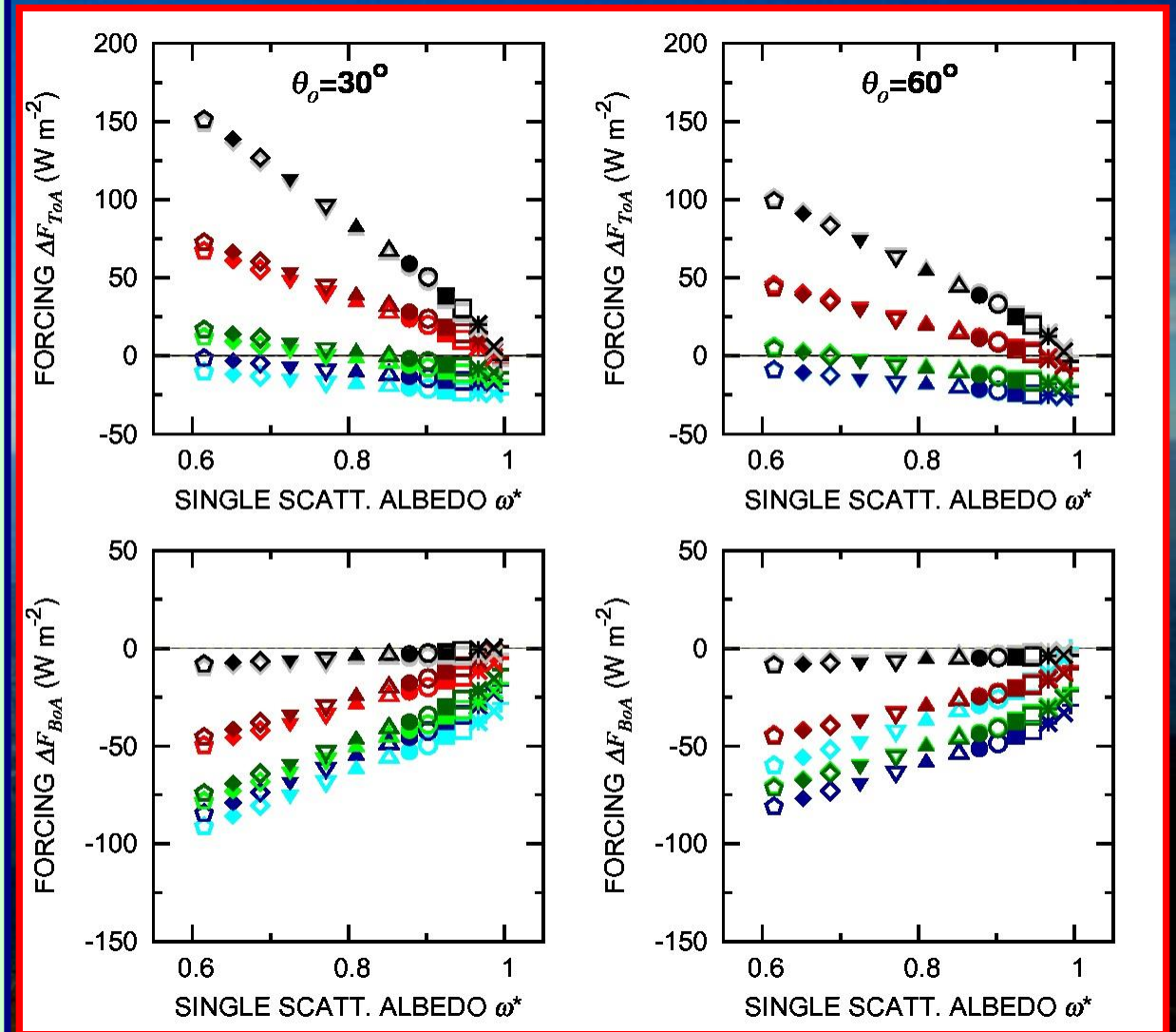

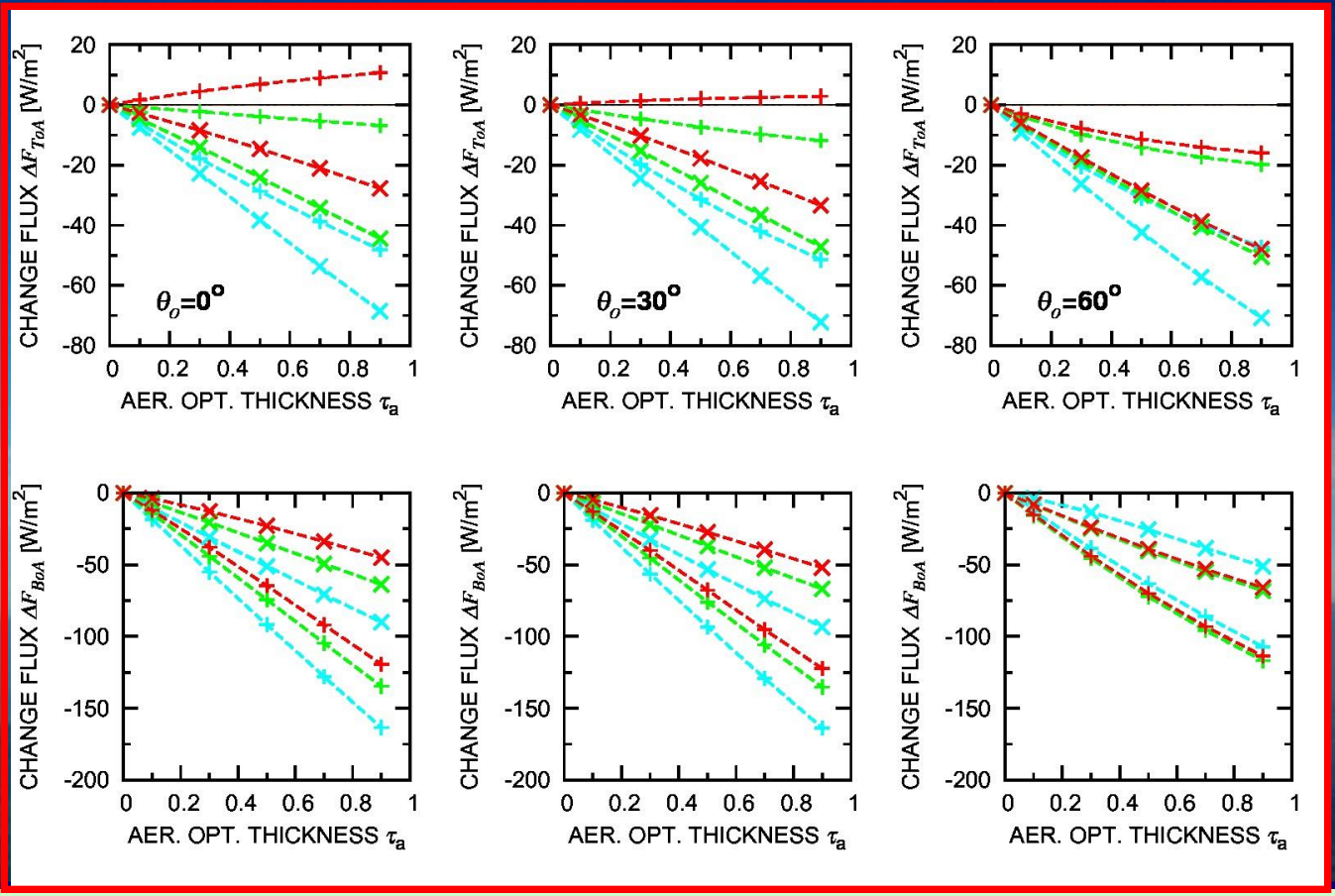

Dependence patterns of instantaneous DARF terms ΔF_{ToA} (upper part), ΔF_{BoA} (lower part) on aerosol optical thickness $\tau_a(0.55\ \mu m)$, for (i) solar zenith angles θ_o equal to 0° (left), 30° (middle) and 60° (right), (ii) the 6S-C continental (+) and the 6S-M maritime (x) aerosol models, and (iii) the oceanic OS2 (cyan), vegetation-covered VS2 (green) and bare-soil BS1 (red) non-Lambertian surface reflectance models.

To study the dependence features of DARF on surface reflectance, a set of 16 non-Lambertian BRDF surface reflectance models was prepared for 4 Oceanic Surface (OS), 4 Vegetated Surface (VS), 4 Bare Soil (BS), and 4 Polar Surface (PS) reflectance models were considered, presenting the spectral curves of white-sky albedo $R_{ws}(\lambda)$ shown in the graph over the wavelength range from 0.4 to 2.5 μm.

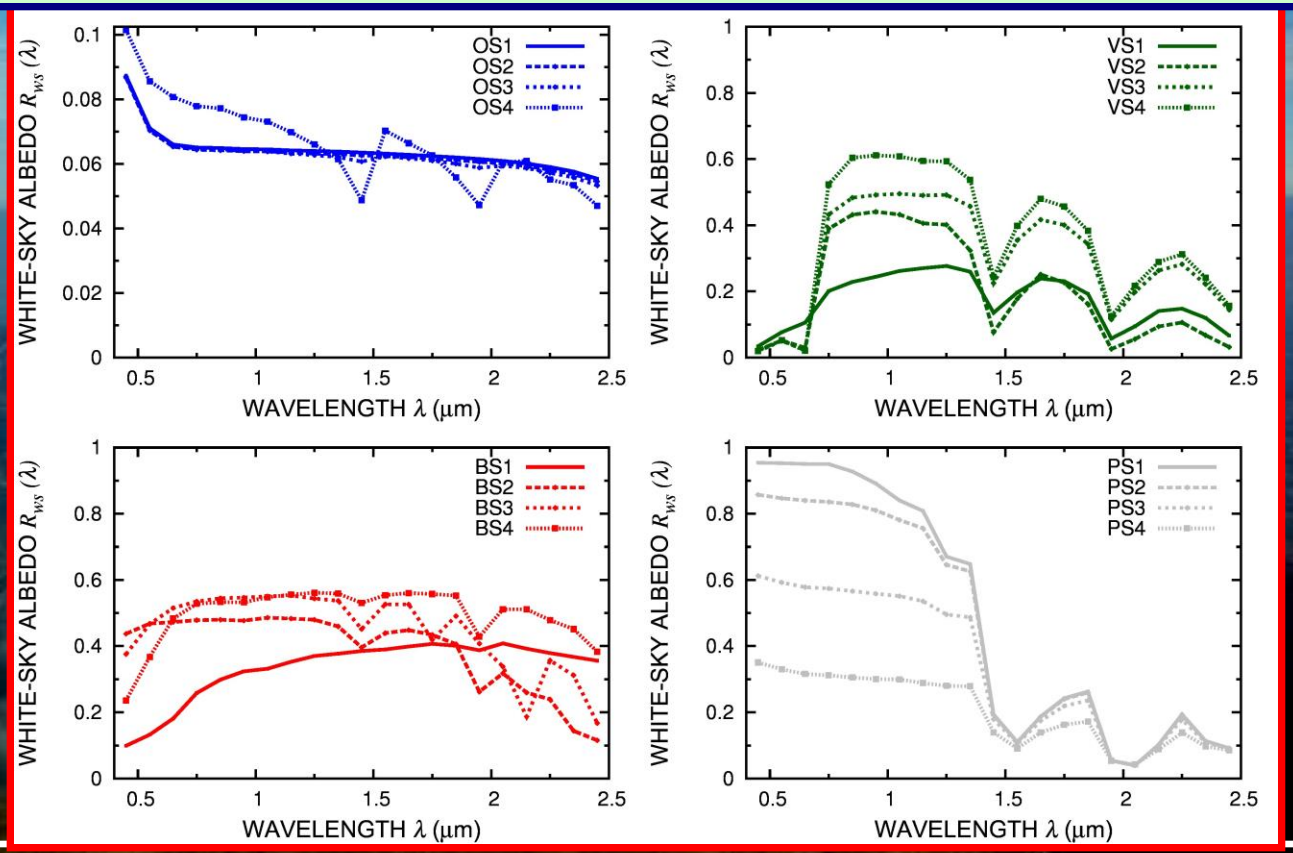

The 16 non-Lambertian BRDF surface reflectance models have been prepared as follows:

(1) The 4 Oceanic Surface (OS) models using the Morel (1988) and Vermote et al. (1997) 6S subroutines for OCEANIC surfaces (including the whitecaps model of Koepke (1984)) for surface wind velocities of 2, 5, 10 and 20 m s^{-1}, sea-water pigment concentration of 0.1 mg m^{-3} and sea-water salt concentration of 34.3 ppt;

(2) The 4 Vegetated Surface (VS) models based on the AK 6S code subroutine adapted to the Kuusk (1994) model and utilizing the PROSPECT code of Jacquemoud and Baret (1990) for simulating the chlorophyll absorption features, and the Nilson and Kuusk (1989) algorithm for representing the reflectance anisotropy characteristics of the one-layer canopy assumed to present LAI values equal to 0.1, 1.5, 2.5 and 5.0, respectively;

(3) The Bare Soil (BS) models based on the BRDF surface reflectance models derived from the non-hyperspectral model of Rahman et al. (1993), giving white-sky albedo values increasing from 0.237 to 0.450;

(4) The Polar Surface (PS) models based on the Wiscombe and Warren (1980) surface characteristics and adapted to the spectral measurements of surface reflectance performed by Lupi et al. (2001) in various Antarctic areas.

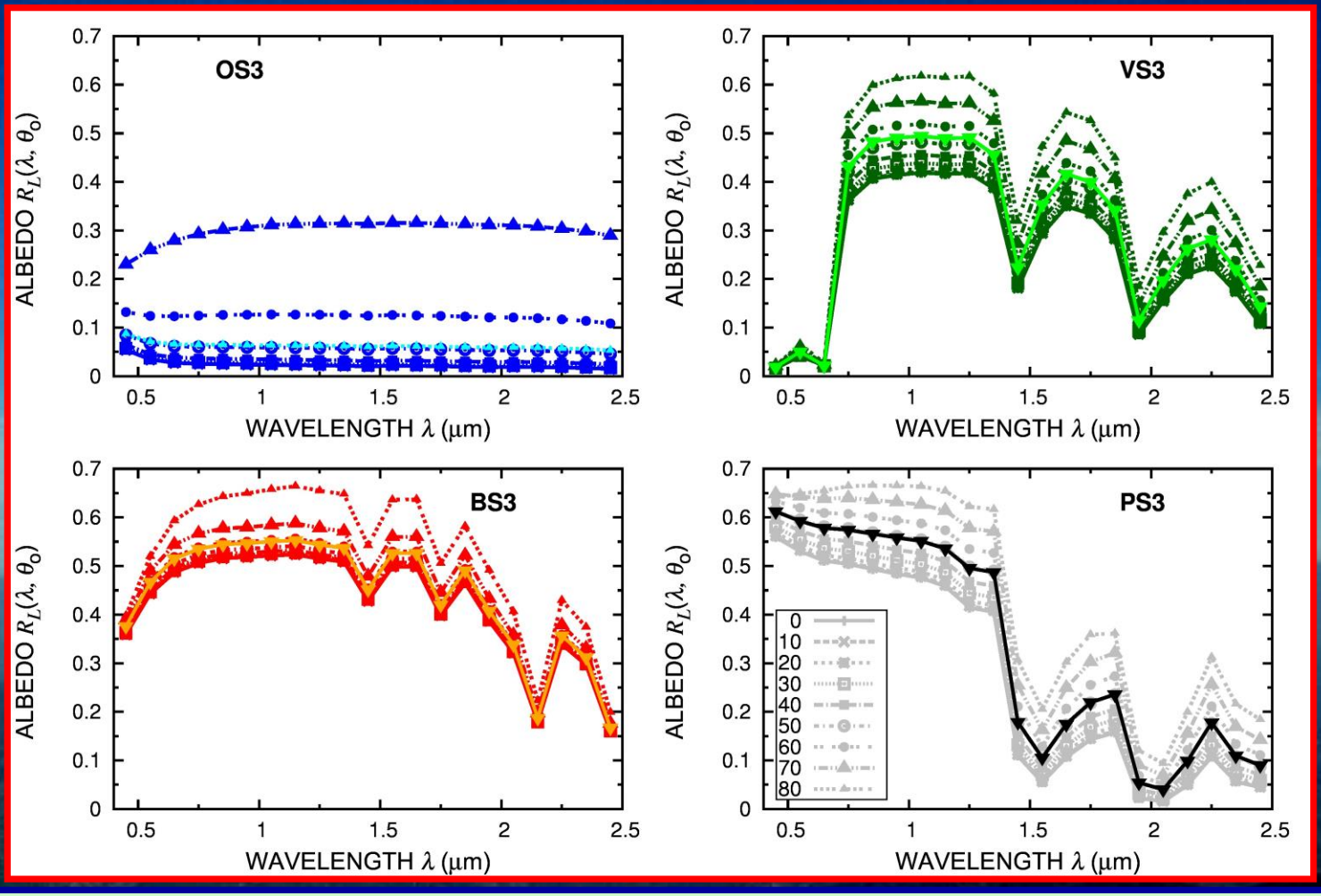

The 16 BRDF surface reflectance models present different spectral curves of surface albedo $R_L(\lambda, \theta_o)$: four of them are shown above over the 0.40 - 2.50 μm wavelength range, obtained for 9 values of solar zenith angle θ_o taken in steps of 10° from 0° to 80°.

The diurnally averaged aerosol forcing terms ΔDF_{ToA} and ΔDF_{BoA} are given by the integrals of instantaneous radiative forcing $\Delta F_{ToA}(t)$ and $\Delta F_{BoA}(t)$ calculated at the ToA- and BoA- levels, respectively, over the sunlit period (from sunrise to sunset) and divided by the 24-hour period, according to the TARFOX procedure adopted by Russell et al. (1999).

The diurnally averaged DARF forcing term in the atmosphere ΔDF_{Atm} has been calculated as the difference between the diurnally averaged DARF terms ΔDF_{ToA} and ΔDF_{BoA}.

This term is not radiative in nature, since it is induced by the thermo-dynamic processes associated with the radiative transfer processes occurring within the aerosol layers: in other words, ΔDF_{Atm} provides a measure of the amount of latent heat released in the atmosphere by aerosol particles (Ramanathan et al., 2001).

The AEROCLOUDS experiment at San Pietro Capofiume in the Po Valley (Nothern Italy)

High concentrations of aerosol particles are often monitored in the Po Valley area throughout the year as shown in the picture made in an autumn day from the Mt, Cimone top, or in the PM2.5 maps derived from MODIS observations.

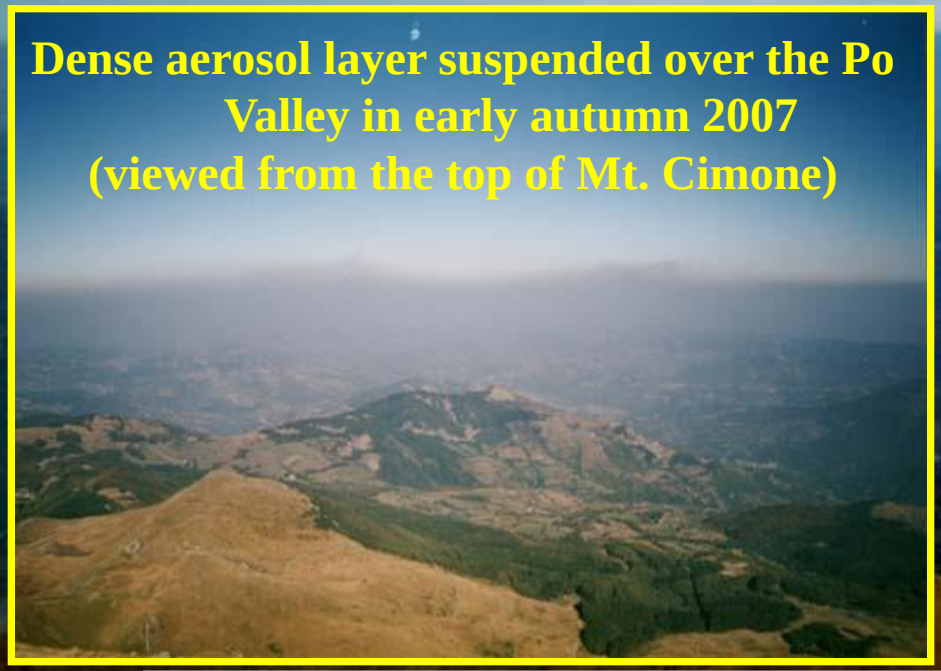

Dense aerosol layer suspended over the Po Valley in early autumn 2007 (viewed from the top of Mt. Cimone)

PM2,5 map from MODIS/Terra data of February 10, 2008 (10:20 UTC) (μg m^{-3})

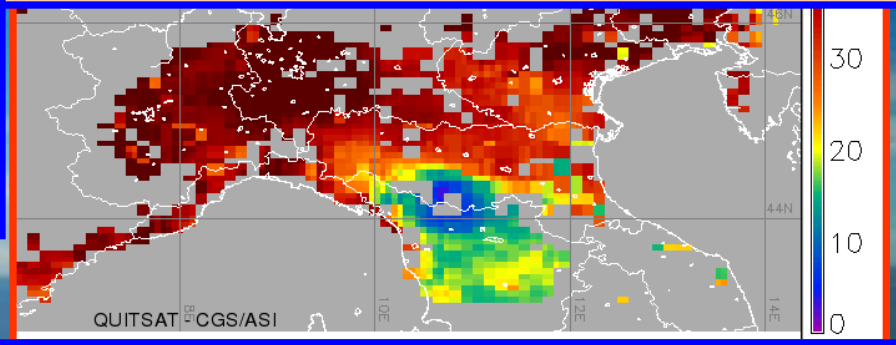

PM2,5 map from MODIS/Aqua data of March 13, 2008 (12:00 UTC) (μg m^{-3})

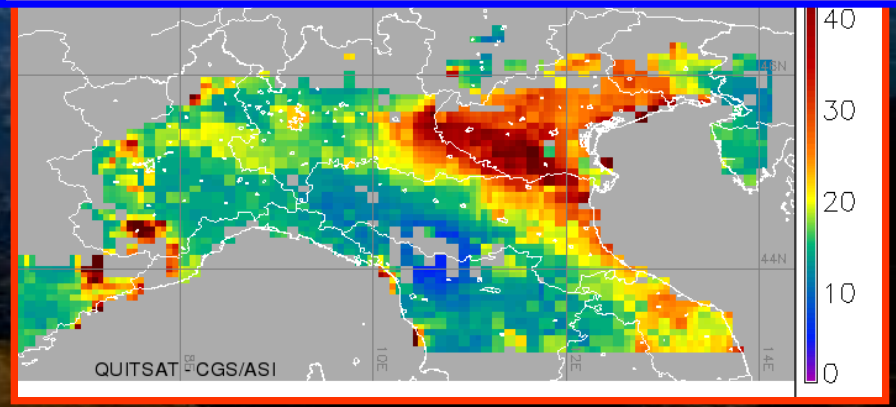

The meteorological station at San Pietro Capofiume (SPC) is managed by ARPA ER.

The PREDE POM-02L Sun/sky-radiometer at SPC

The PREDE sun/sky-radiometer, model POM-02L, placed at San Pietro Capofiume (Po Valley) in Northern Italy (about 25 km NE from Bologna), is one of the Sun/ Sky-radiometers of the SKYNET network in Europe.
Routine measurements are performed on clear-sky days of: (i) the spectral values of aerosol optical thickness at the 315, 340, 380, 400, 500, 675, 870, 1020, 1600, and 2200 nm wavelengths, (ii) Ångström's exponent α over the 0.40-0.87 μm wavelength range, (iii) precipitable water, and (iv) Level 2.0 measurements of complex refractive index, asymmetry factor, and single scattering albedo derived from the sky-brightness measurements in the almucantar.

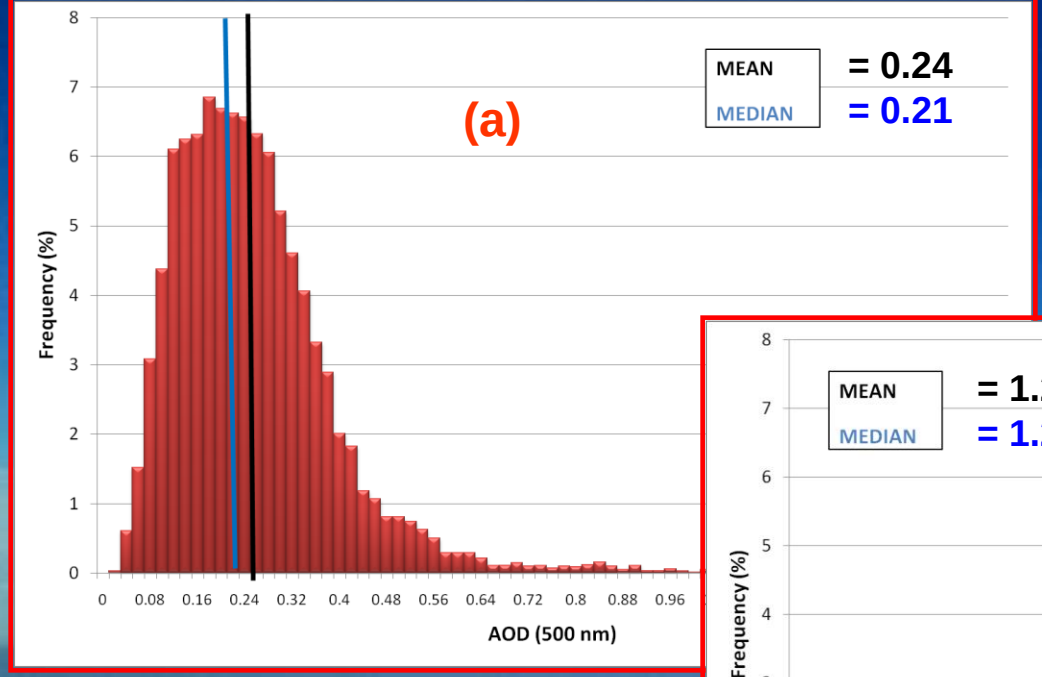

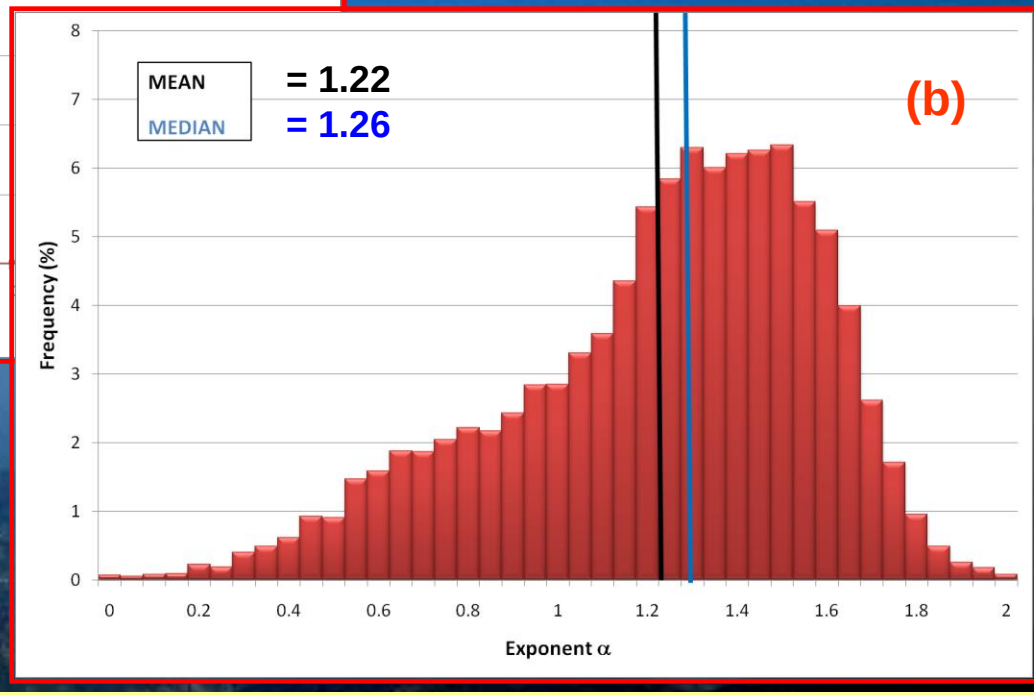

Relative frequency histograms of (a) daily average values of aerosol optical thickness $\tau_a(0.50\ \mu m)$, and (b) the daily average values of Ångström exponent $\alpha(0.40\text{-}0.87\ \mu m)$ measured at SPC from May 2007 to late May 2010 using the PREDE POM-02L sun/sky-radiometer.

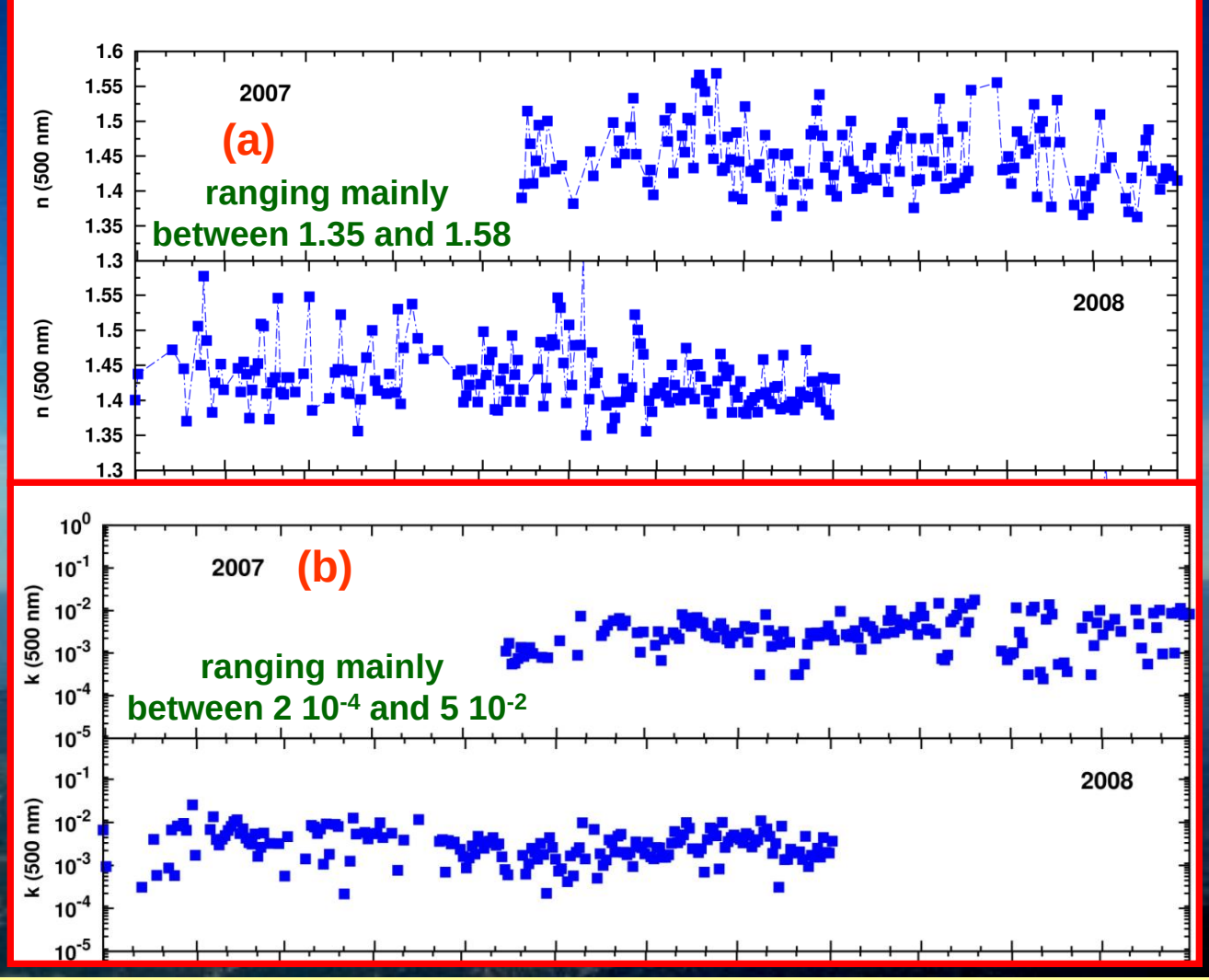

Time patterns of the daily mean values of (a) real part *n(0.50 μm)* and (b) imaginary part *k(0.50 μm)* of the columnar aerosol refractive index retrieved from the sky-brightness in the almucantar measurements performed at SPC in 2007 and 2008 using the PREDE POM-02L sun/sky-radiometer.

AEROCLOUDS experiment

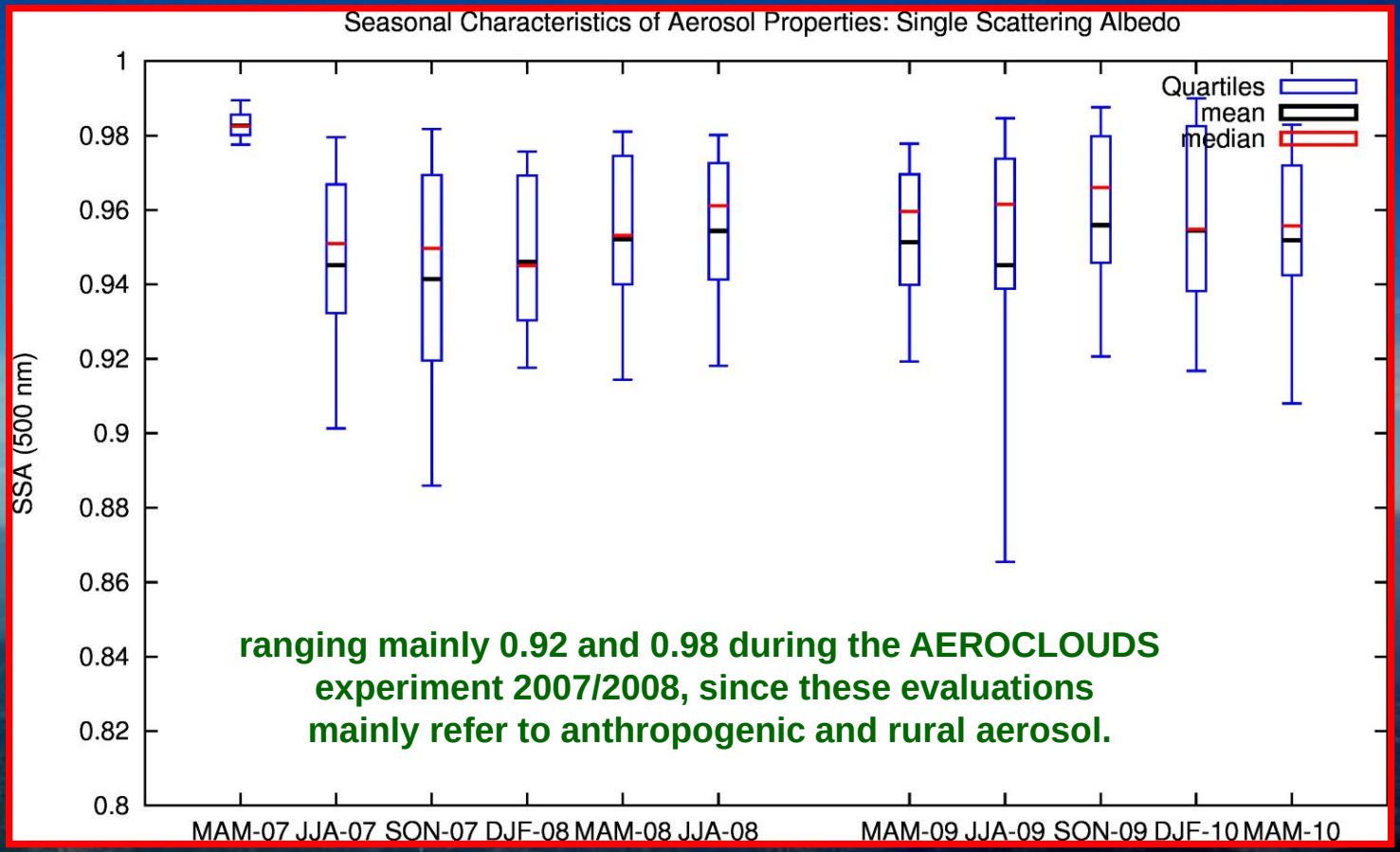

Seasonal mean values (black bars), median (red bars) and 10th, 25th, 75th and 90th percentile (blue bars) of columnar aerosol single scattering albedo $\omega(0.50\ \mu m)$, derived from the sky-brightness measurements in the almucantar performed at San Pietro Capofiume (Po Valley) from half May 2007 to late May 2010.

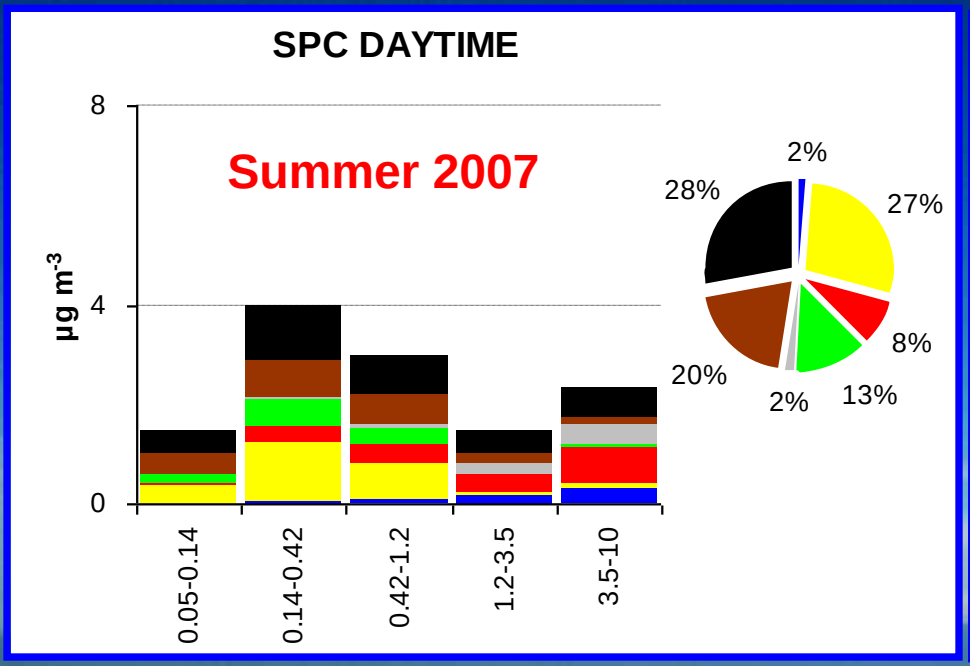

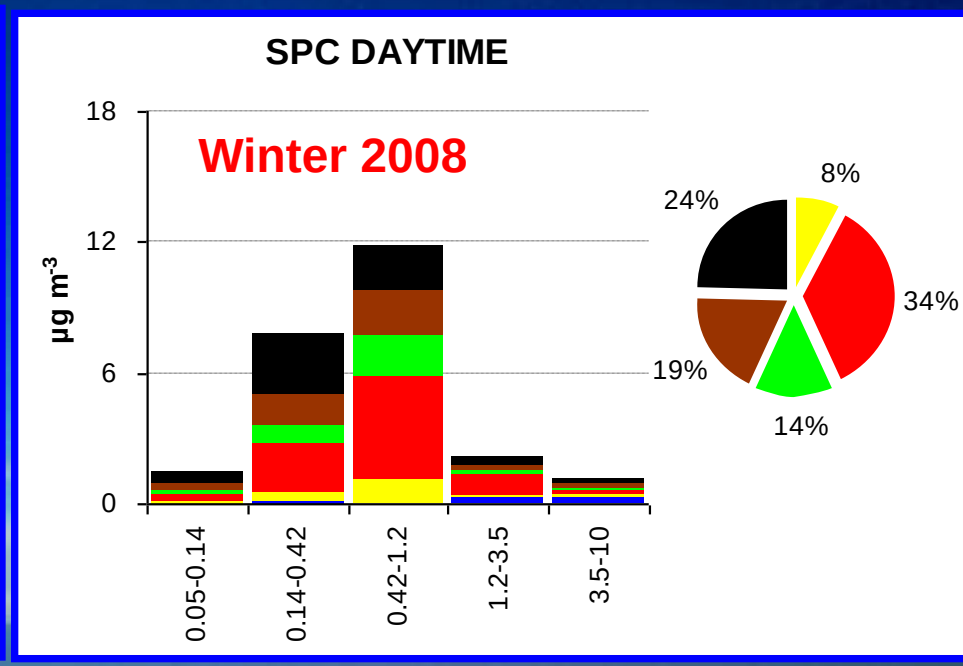

Day-time size-segregated aerosol composition of fine particles (first three classes from 0.05 to 1.2 µm diameter) and coarse particles (last two classes from 1.2 to 10 µm diameter) measured in summer 2007 (left) and winter 2008 (right) at SPC, with the percentages of the various aerosol constituents (Carbone et al., 2010).

Azure colour refers to sea-salt particles,
Red to nitrate ions,
Gray to calcium ions,
Yellow to sulphate ions,
Green to ammonium ions,
Brown to water-soluble organic matter,
Black to water-insoluble carbonaceous matter.

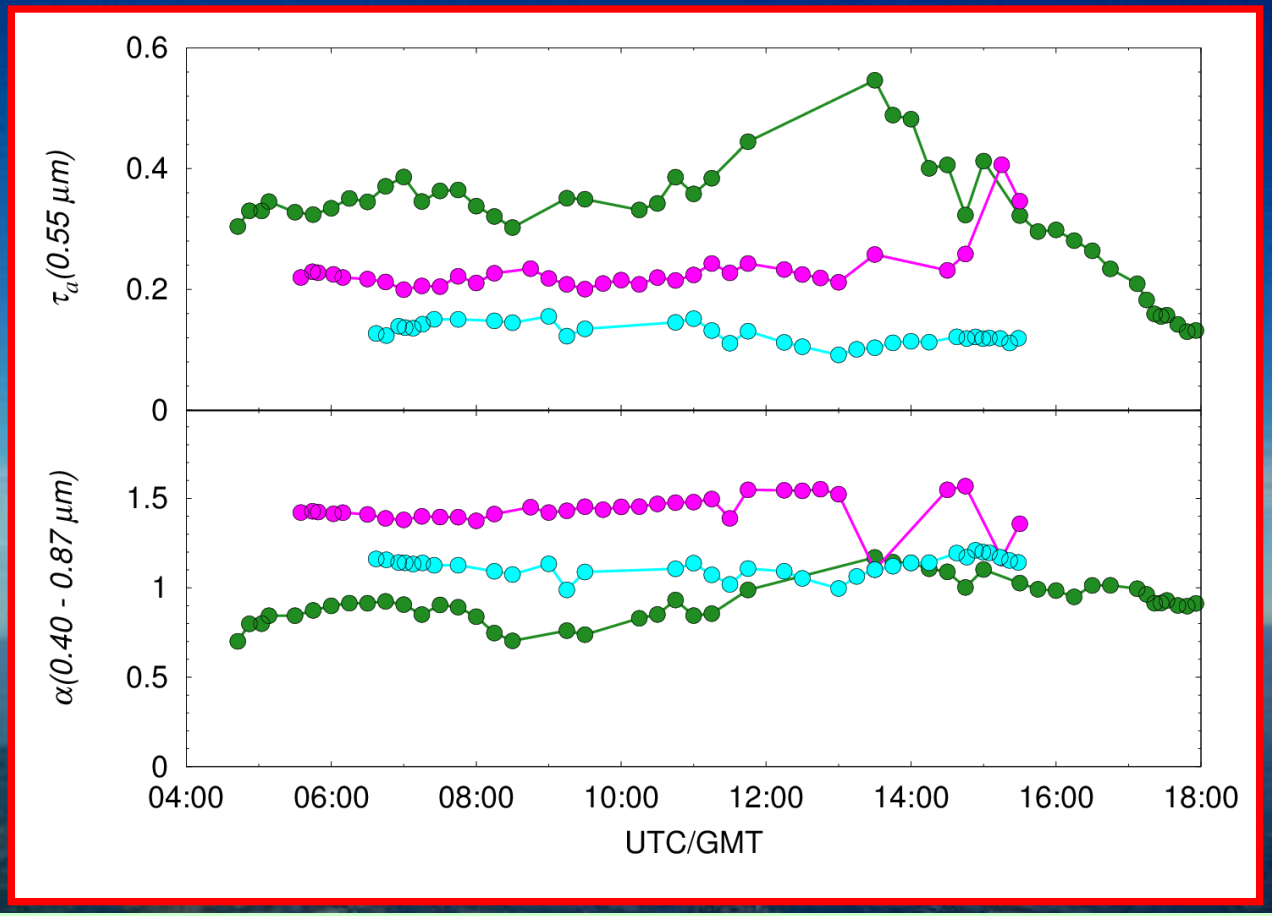

Examples of time-patterns of $\tau_a(0.55\ \mu m)$ (upper part) and Ångström's exponent $\alpha(0.40\text{-}0.87\mu m)$ derived at SPC on June 21, 2007 (anthropogenic aerosol with Saharan dust) (dark green circles)), August 19, 2007 (continental aerosol from North-western Europe (fuchsia circles)), and October 15, 2007 (continental aerosol from the Arctic and Northern European regions (cyan circles)).

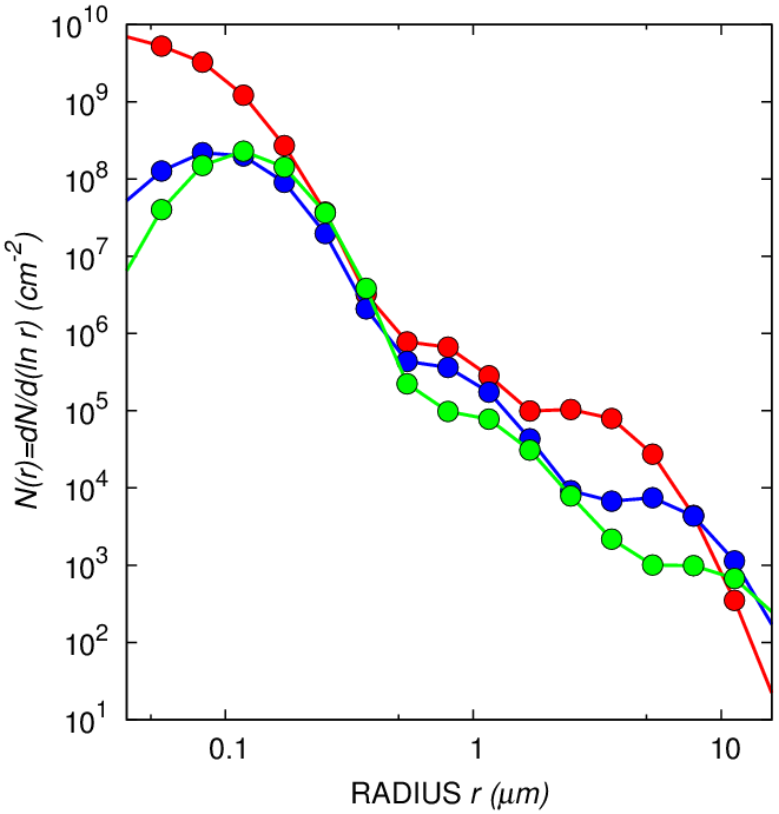

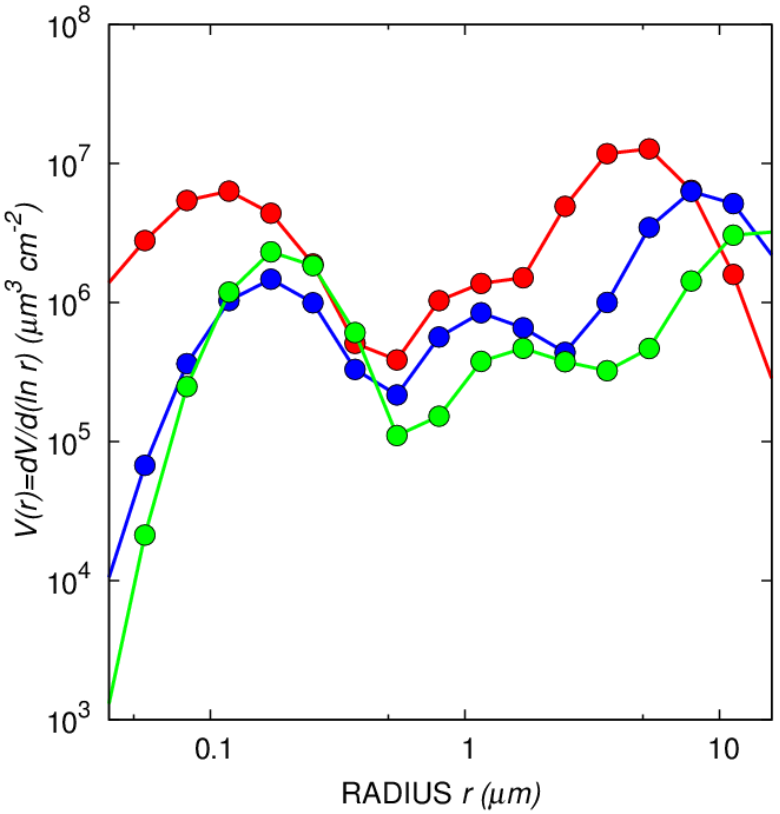

Multimodal size-distribution curves of columnar total particle number density *N(r)* = d*N*/d(ln *r*) measured in cm^{-2} (left) and columnar total particle volume *V(r)* = d*V*/d(ln *r*) measured in μm^3 cm^{-2} (right), as retrieved using the SKYRAD 5.0 code from the PREDE POM-02L spectral series of $\tau_a(\lambda)$ determined at SPC on the following three AEROCLOUDS golden days: (a) July 1, 2007 (07:45 UTC) for mixed marine/continental aerosol from Atlantic Ocean, Southern France and Ligurian Sea (α = 1.347) (red circles); (b) October 15, 2007 (11:45 UTC) for continental aerosol from Arctic and Northern Europe with α = 1.107 (blue circles); and (c) December 19, 2007 (08:22 GMT) for continental aerosol from Eastern Europe (α = 1.694) (green circles).

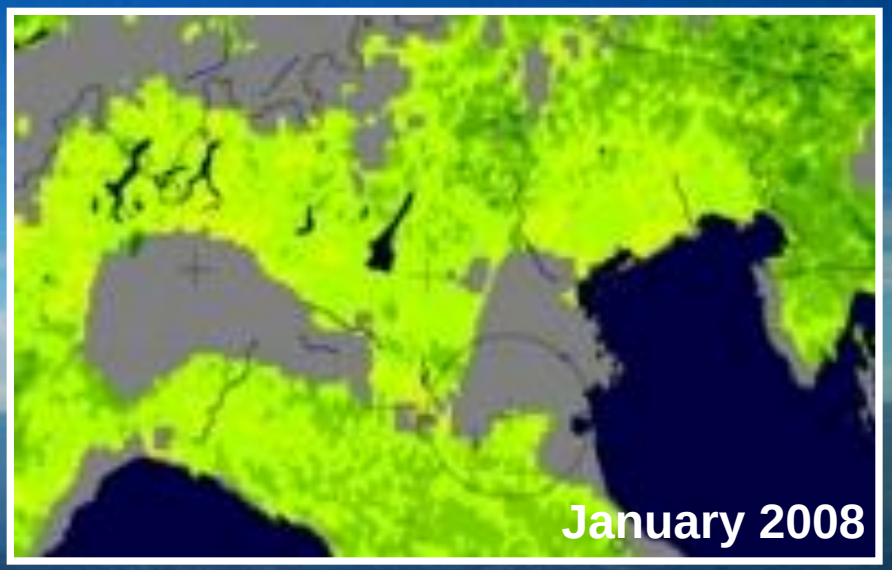

Monthly mean maps of Normalized Difference Vegetation Index (NDVI) over Northern Italy determined from MISR/Terra observations performed in August 2007 (left) and January 2008 (right), providing evidence of the strong seasonal variations in the surface reflectance characteristics occurring from summer to winter. Gray colour in the right graph are due to the presence of thin snow layers covering the surface.

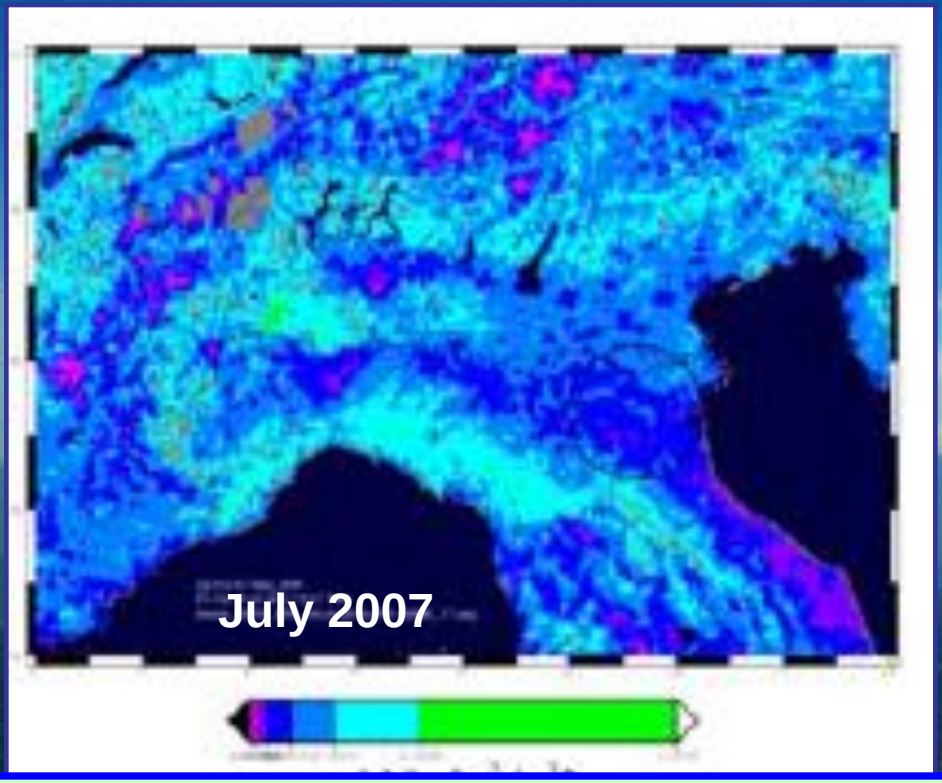

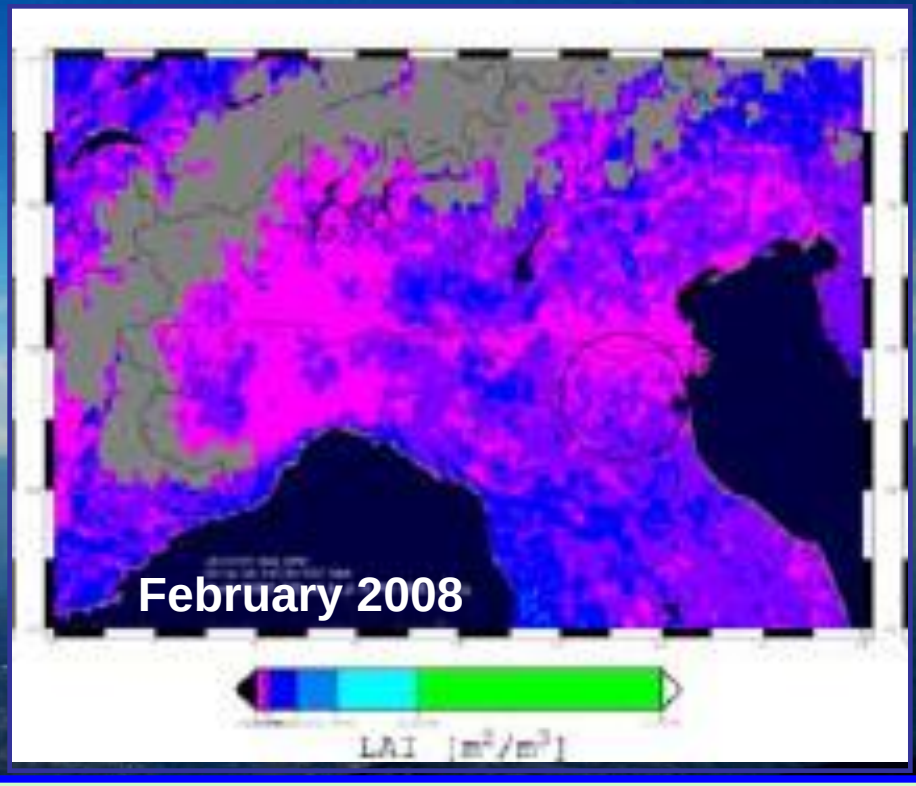

Monthly mean maps of Leaf Area Index (LAI) obtained in July 2007 (left) and in February 2008 (right) over the Alps and Northern Italy. Grey colour in the right graph marks the Alpine areas covered by snow in late winter. Black circles individuate the area surrounding the SPC measurement station.

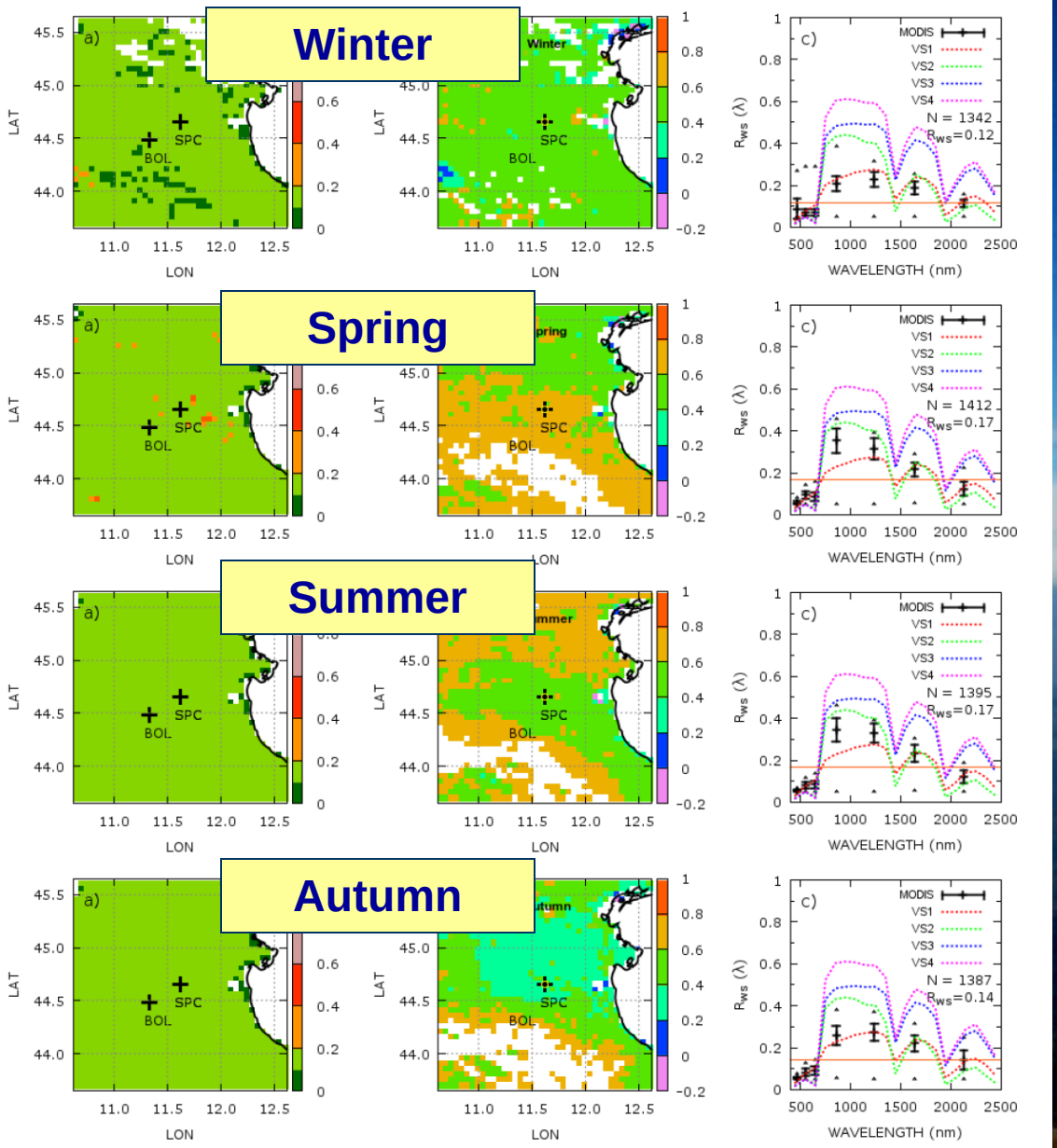

Average seasonal maps of the land surface albedo (left column) and NDVI (middle column) derived over the eastern part of the Po Valley area (Northern Italy) from the MODIS Level 3.0 surface albedo data (MCD43C3 products) recorded during the four seasonal periods.

The graphs in the third column provide the spectral values (black vertical bars) of the white-sky albedo R_{ws} over land, yielding mean values of 0.12 in winter, 0.17 in spring and summer, and 0.14 in autumn, all found with standard deviations of around 0.1 within all the seven MODIS channels, for which the small triangles yield the spectral minima and maxima. The graphs also show the spectral curves of $R_{ws}(\lambda)$ obtained as best-fit solutions for the four VS surface albedo models.

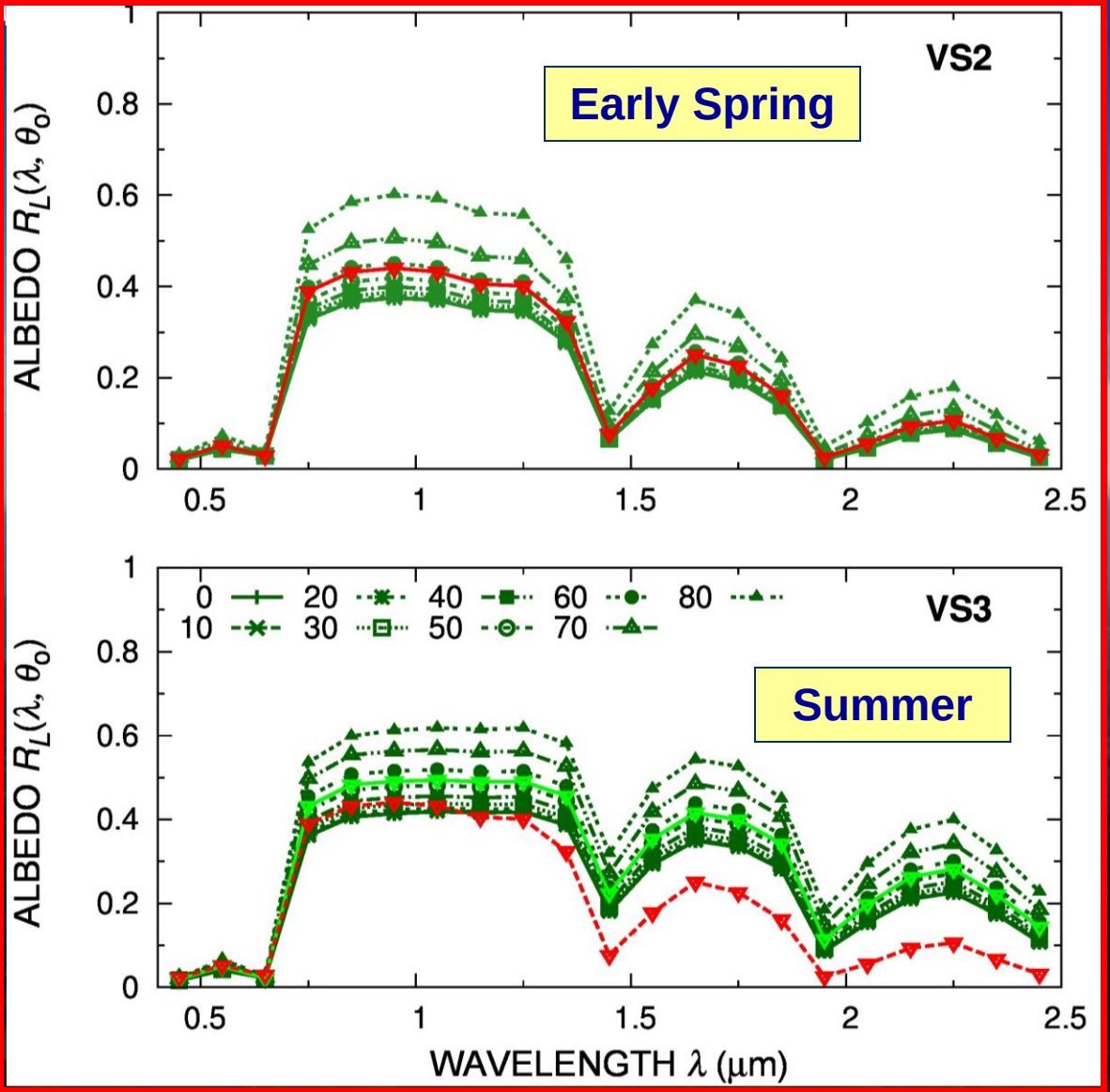

Spectral curves of the BRDF surface albedo $R_L(\lambda, \theta_o)$ defined by Tomasi et al. (2013) for the vegetation-covered surface albedo models VS2 and VS3, evaluated for nine values of solar zenith angle θ_o, taken in steps of 10° over the 0°-80° range, over the eastern part of the Po Valley around SPC station in Northern Italy. Model VS2 refers to a vegetation-covered surface with LAI = 1.5, and model VS3 to a vegetation-covered surface with LAI = 2.5. Red spectral curves provide the white-sky albedo $R_{ws}(\lambda)$ for the VS2 model, and light green curve the curve of $R_{ws}(\lambda)$ of the VS3 model.

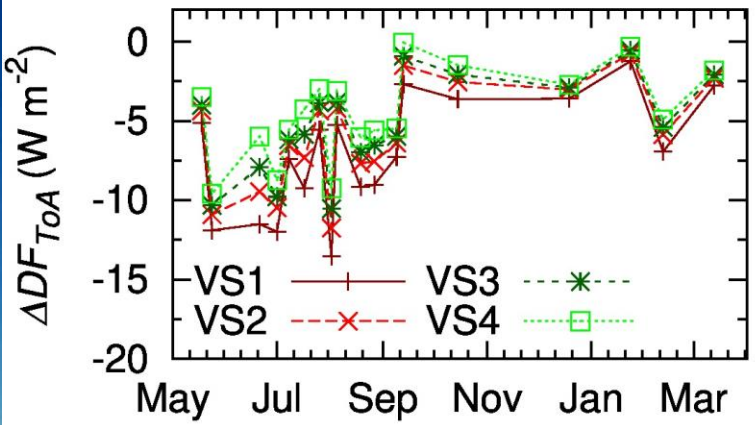

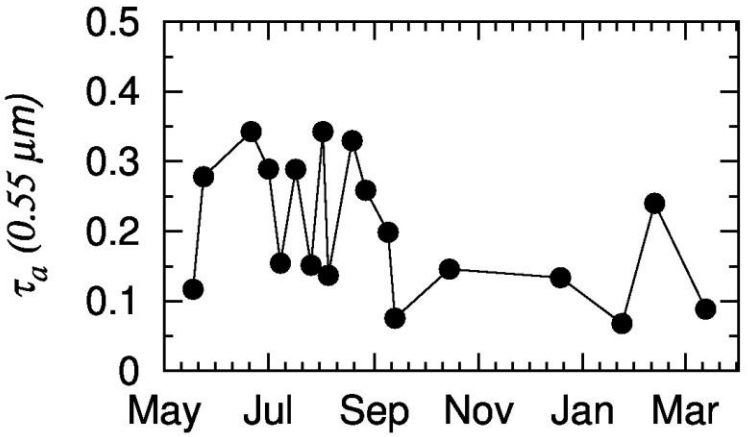

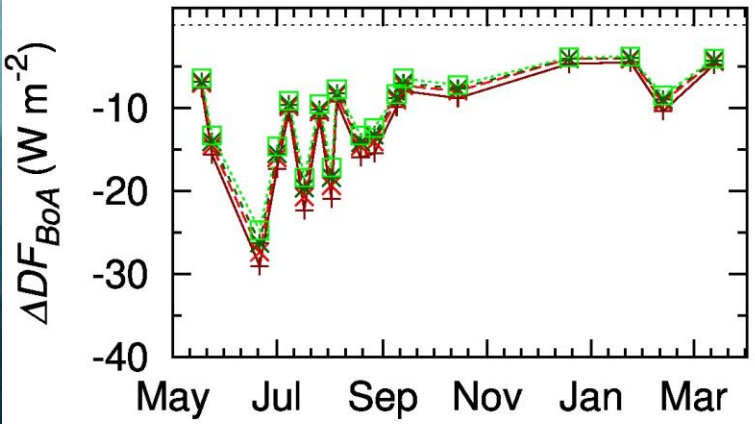

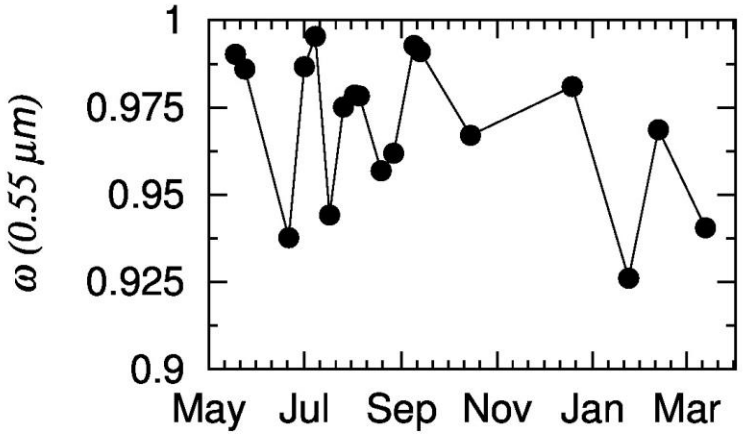

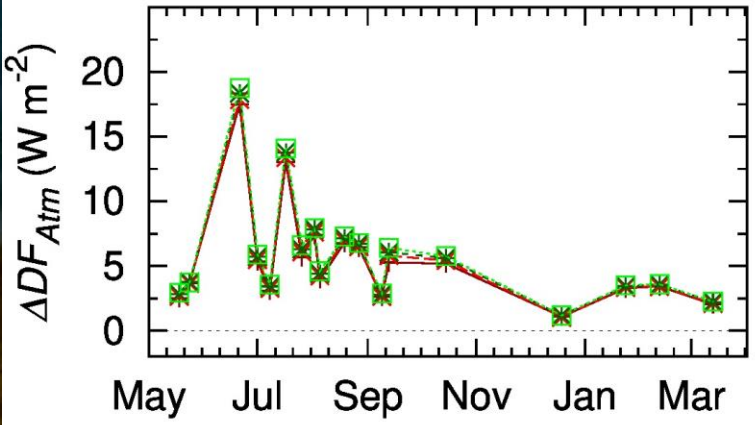

Left: Time-patterns of the daily mean values of diurnally averaged DARF terms ΔDF_{ToA}, ΔDF_{BoA}, and ΔDF_{Atm} calculated for the 18 AEROCLOUDS golden days at SPC, using the vegetation-covered surface albedo models VS1, VS2, VS3, and VS4 defined by Tomasi et al. (2013). Right: Correspond-ing time-patterns of the daily mean values of aero-sol optical thickness τ_a(0.55 µm) and columnar aerosol single scattering albedo ω(0.55 µm).

For *SSA* ranging from 0.92 to 1.00

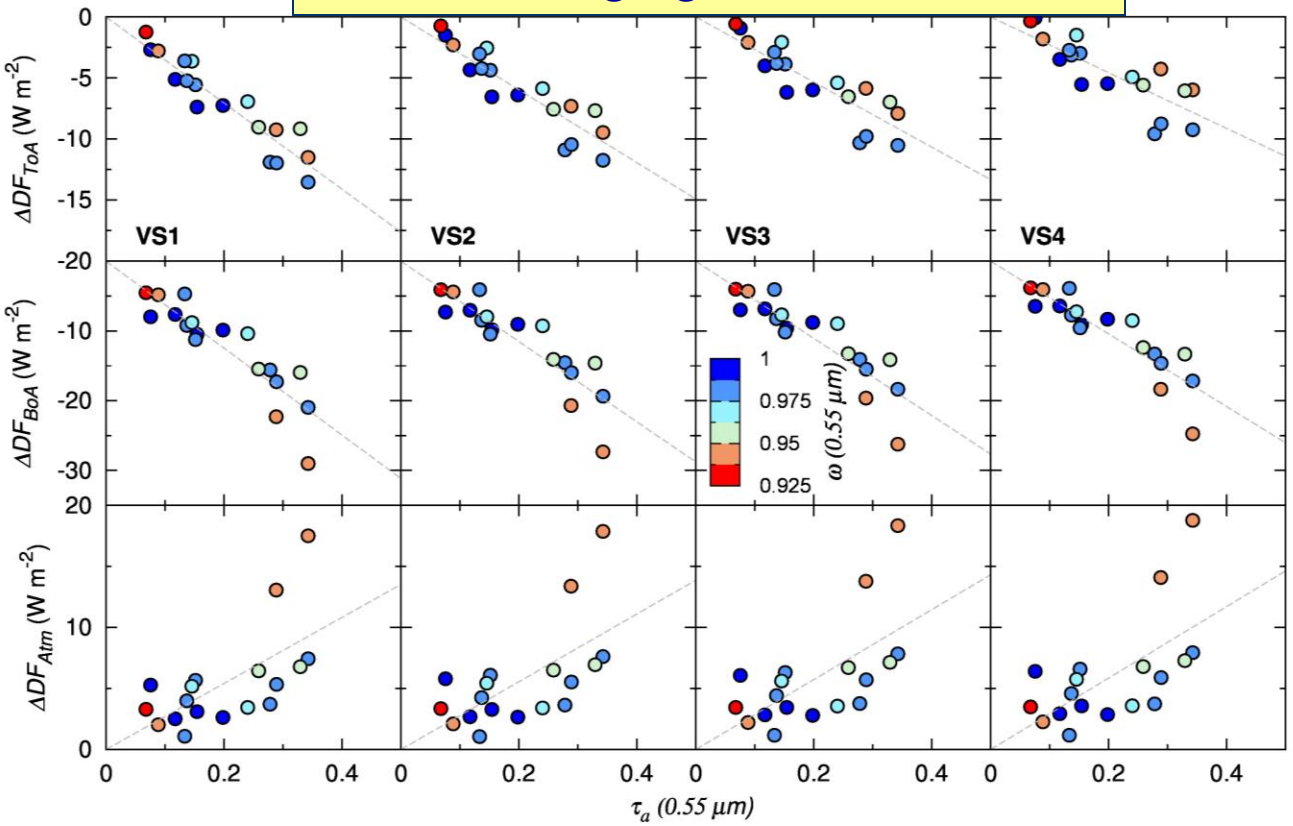

Scatter plots of the diurnally averaged values of ΔDF_{ToA}, ΔDF_{BoA} and ΔDF_{Atm} versus the daily mean values of $\tau_a(0.55\ \mu m)$, as determined for the 18 AEROCLOUDS golden days using the four vegetation-covered surface albedo models VS1, VS2, VS3 and VS4, and for different values of columnar aerosol $\omega(0.55\ \mu m)$, indicated by circles of different colours over the 0.925-1.000 range of SSA.

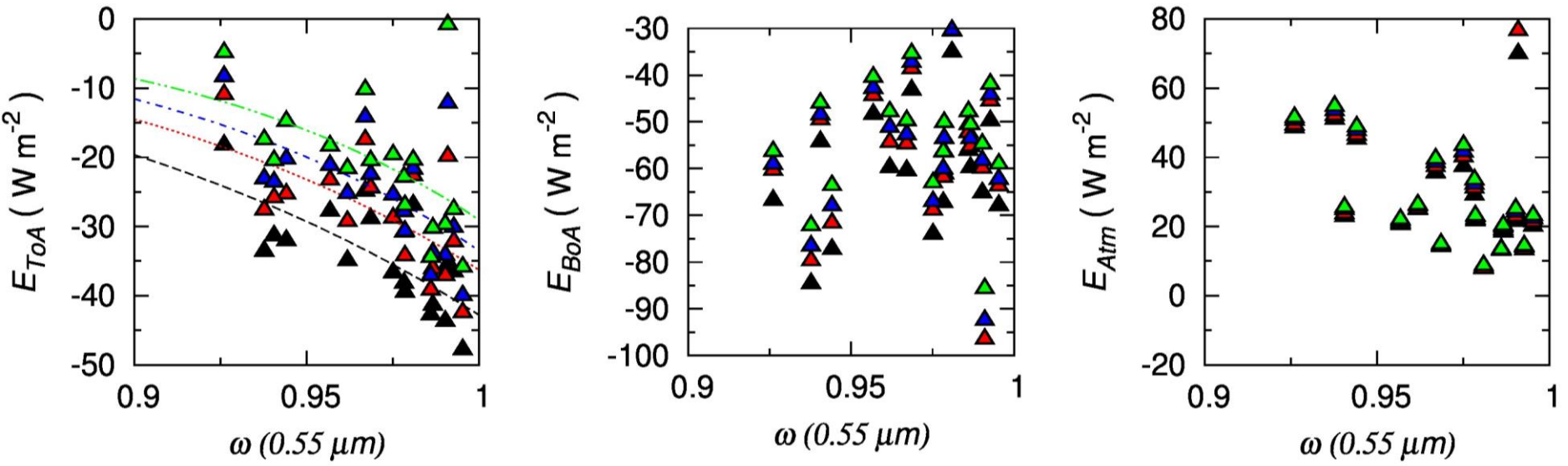

Scatter plots of the daily mean values of DARF efficiency E_{ToA} at the ToA-level, DARF efficiency E_{BoA} at the BoA-level, and DARF efficiency E_{Atm} within the atmosphere versus the columnar aerosol single scattering albedo $\omega(0.55\ \mu m)$, as obtained on the 18 golden days of the AEROCLOUDS experiment conducted at San Pietro Capofiume (SPC, Po Valley, Northern Italy) from May 2007 to March 2008, by assuming the surface albedo characteristics represented by the vegetation-covered surface albedo models VS1 (black triangles), VS2 (red triangles), VS3 (blue triangles), and VS4 (green triangles).

Conclusions

Examining the results obtained from the field measurements performed during the following experiments conducted in mid-latitude regions:

(1)CLEARCOLUMN (ACE-2) experiment in Southern Portugal (summer 1997);

(2) PRIN-2004 experiment at Lecce (Puglia, Southern Italy) (2003/04);

(3) AEROCLOUDS experiment at San Pietro Capofiume (Po Valley, Northern Italy) (May 2007- March 2008);

(4) Aerosols99 cruise across the Atlantic Ocean (January 1999); and

(5) DOE/ARM/AIOP project in North-central Oklahoma (USA) (May 2003),

for various maritime aerosol and continental aerosol types over sea and land (represented by the OS and VS surface reflectance models), the efficiency parameters were found to vary as a function of columnar aerosol single scattering albedo with average slope coefficients that are considerably higher over land than those over sea.

Scatter plots of the daily mean values of DARF efficiencies E_{ToA} at the ToA-level, E_{BoA} at the BoA-level, and E_{Atm} in the atmosphere shown versus the columnar aerosol single scattering albedo $\omega(0.55\ \mu m)$ over oceanic/sea (left) and land surfaces (right), for different aerosol types:

Pure marine and marine-continental clean (circles);
Mixed maritime/continental polluted (squares);
Mixed maritime/Saharan dust (triangles);
Mixed maritime/forest fire smoke (diamonds).
Different colours mark the OS and VS surface albedo models.

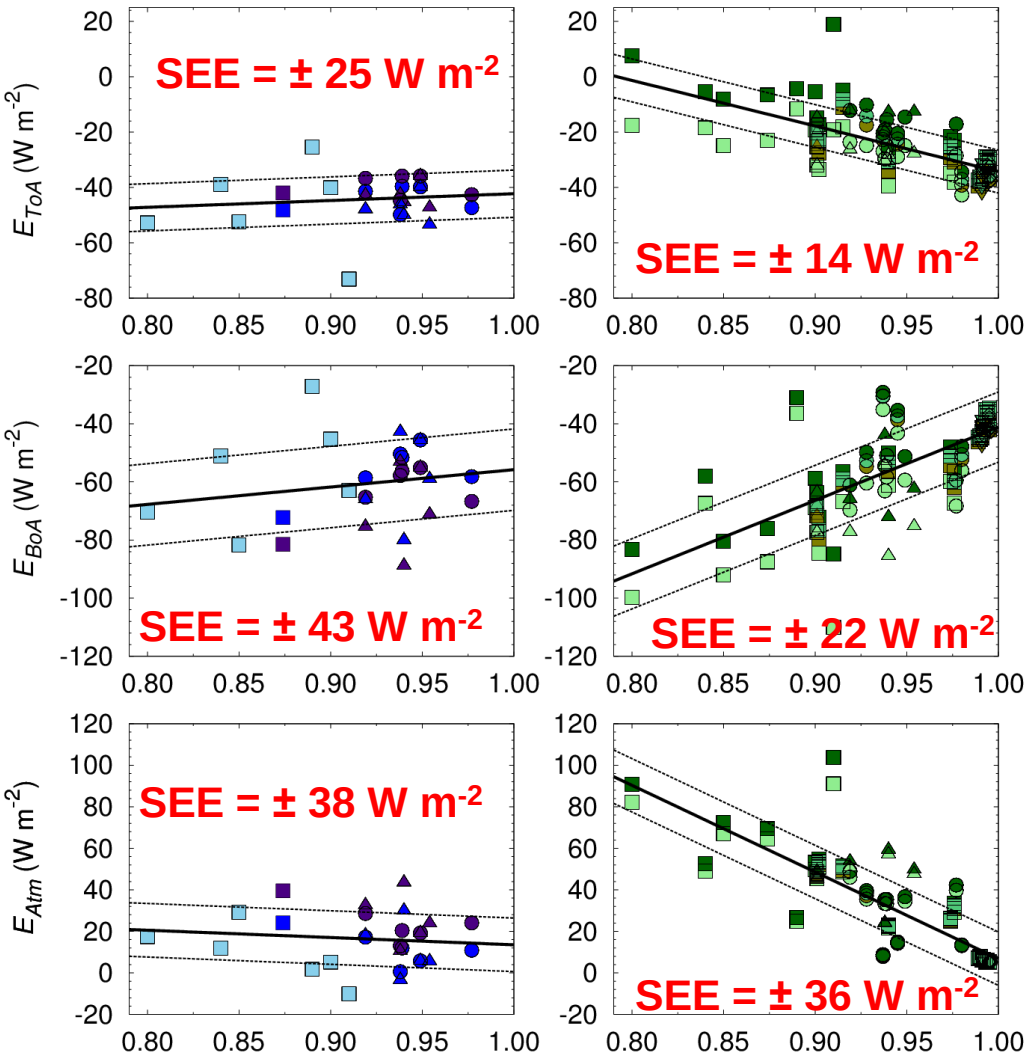

Scatter plots of the daily mean values of DARF efficiencies E_{ToA} at the ToA-level, E_{BoA} at the BoA-level, and E_{Atm} in the atmosphere shown versus the columnar aerosol single scattering albedo $\omega(0.55\ \mu m)$ over oceanic/sea (left) and land (right) surfaces, for different aerosol types:

Continental clean (circles);
Continental polluted (squares);
Continental and forest fire smoke (diamonds);
Continental polluted/Saharan dust (upward triangles);
Continental clean with mineral dust (downward triangles).
Different colours mark the OS and VS surface albedo models

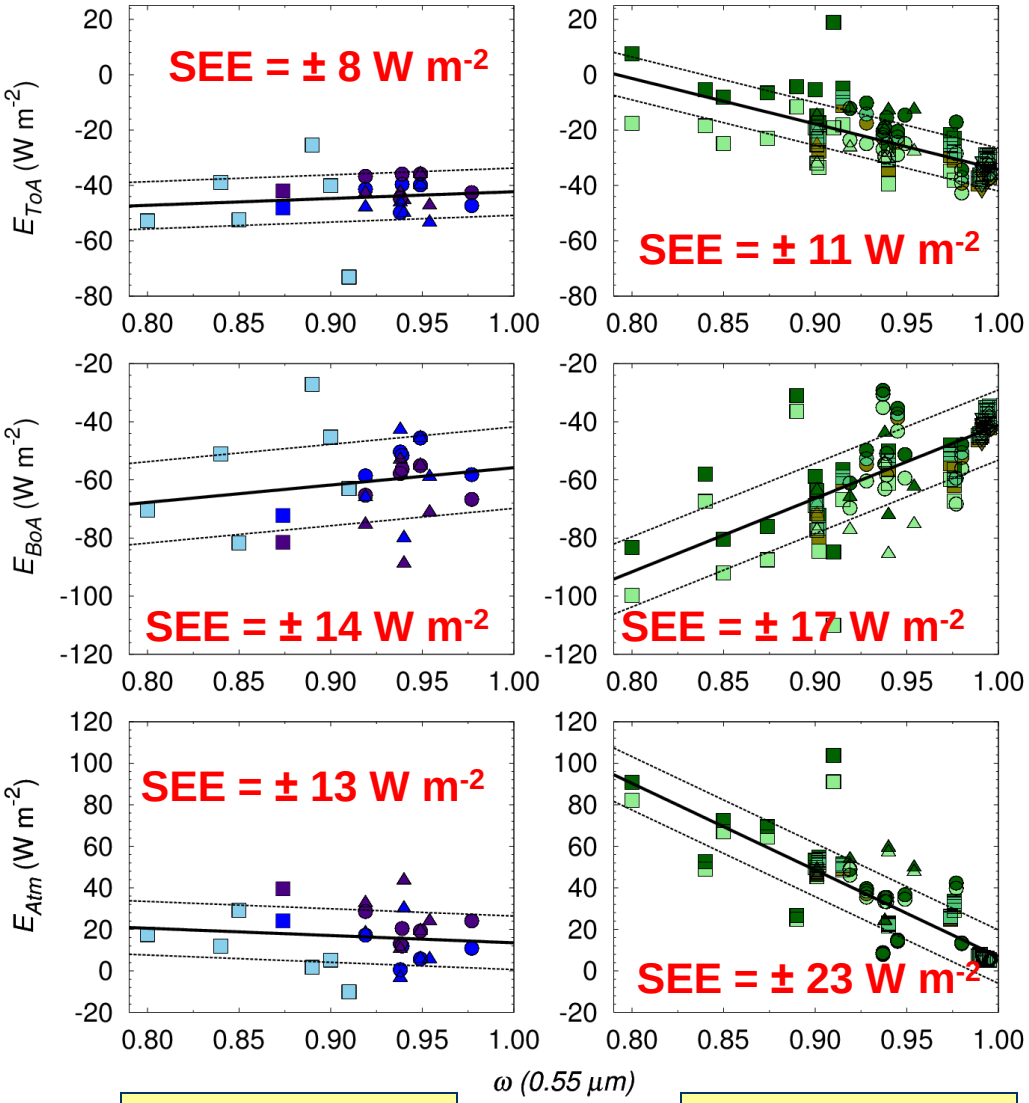

The large scatter of data is only in part due to the different aerosol types considered and can be mainly attributed to the different surface albedo characteristics.

The results clearly indicate that correct DARF evaluations can be made using:
(1) Realistic aerosol extinction models, to represent the columnar aerosol load, which consists often of different aerosol types forming distinct layers; and
(2) Non-Lambertian BRDF surface reflectance models chosen on the basis of satellite observations, to represent the reflectance characteristics of the underlying surface.

Thank you for your kind attention

E-mail: c.tomasi@isac.cnr.it

Workshop on “Remote sensing of atmospheric aerosol, clouds, and aerosol-cloud interactions“, Bremen, December 16 – 19, 2013

Workshop on “Remote sensing of atmospheric aerosol, clouds, and aerosol-cloud interactions“, Bremen, December 16 – 19, 2013

Workshop on “Remote sensing of atmospheric aerosol, clouds, and aerosol-cloud interactions“, Bremen, December 16 – 19, 2013

Among the 14 so-called M-type aerosol models proposed by Tomasi et al. (2013, LSR Volume 8):

Model M-1 consists of pure oceanic aerosol particles;

Model M-2 consists of maritime particles only.

Model M-3 to M-7 are given by linear combinations of decreasing percentage mass concentrations of maritime aerosol particles and gradually increasing per-centages of continental aerosol particles.

Model M-8 consists of continental particles only.

Models M-9 to M-11 of continental polluted aerosols.

Models M-12 and M-13 of anthropogenic-continental aerosols.

Model M-14 of heavy polluted aerosols.

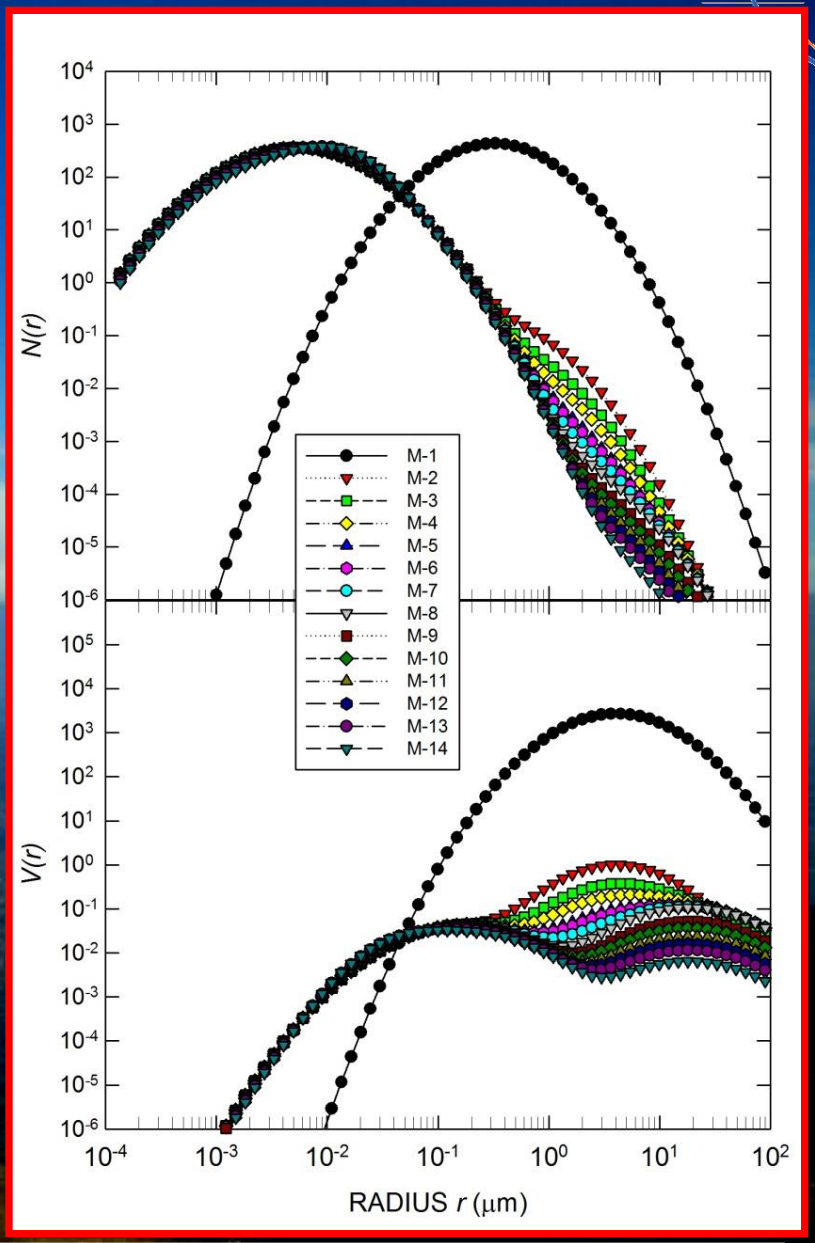

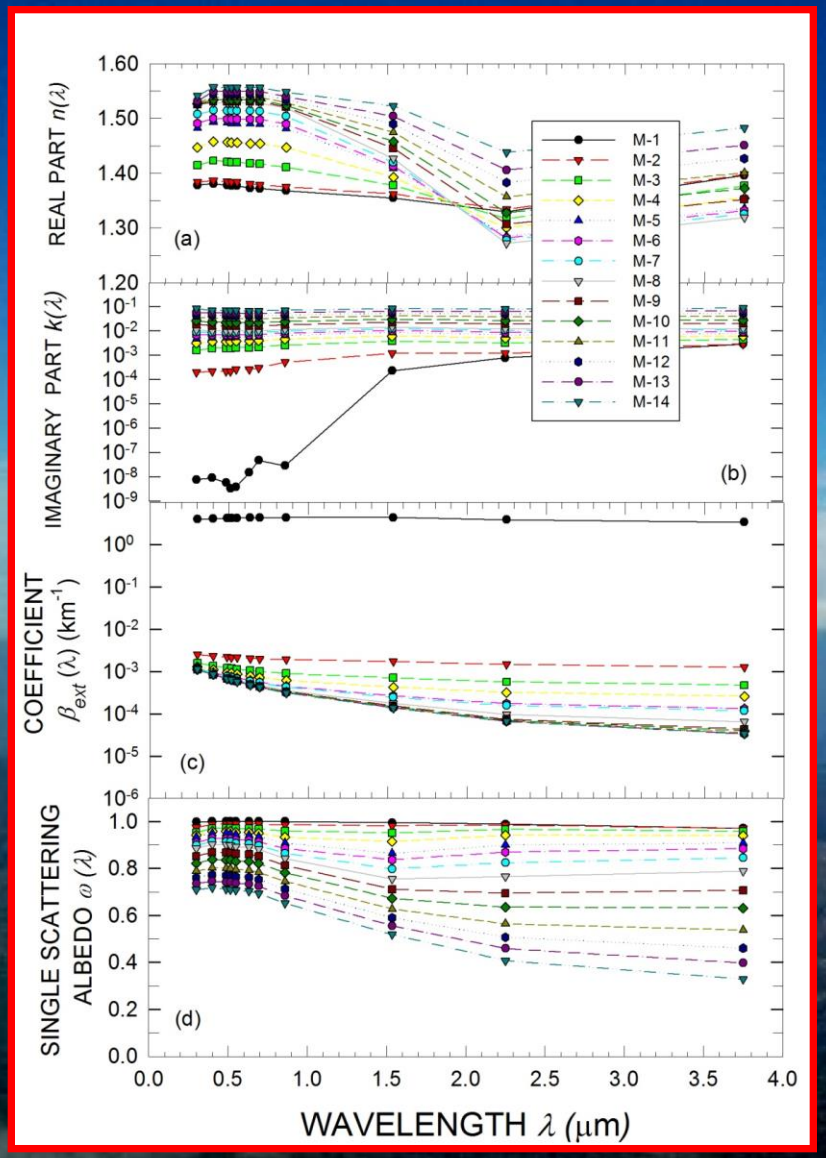

Refractive index real part *n(0.55 μm)* varies between 1.38 and 1.57.

Refractive index imaginary part *k(0.55 μm)* varies between 10^{-8} (M-1) and 0.1 (M-14).

Single scattering albedo *ω(0.55 μm)* was evaluated to vary between less than 0.70 (M-14) and 1.0 (M-1).

M-type aerosol models of Tomasi et al. (2013)

Level 2.0 AOD and SSA time-patterns recorded in September 2007

Aerosol optical thickness at 0.34, 0.38, 0.40, 0.50, 0.675, 0.87, and 1.02 µm.

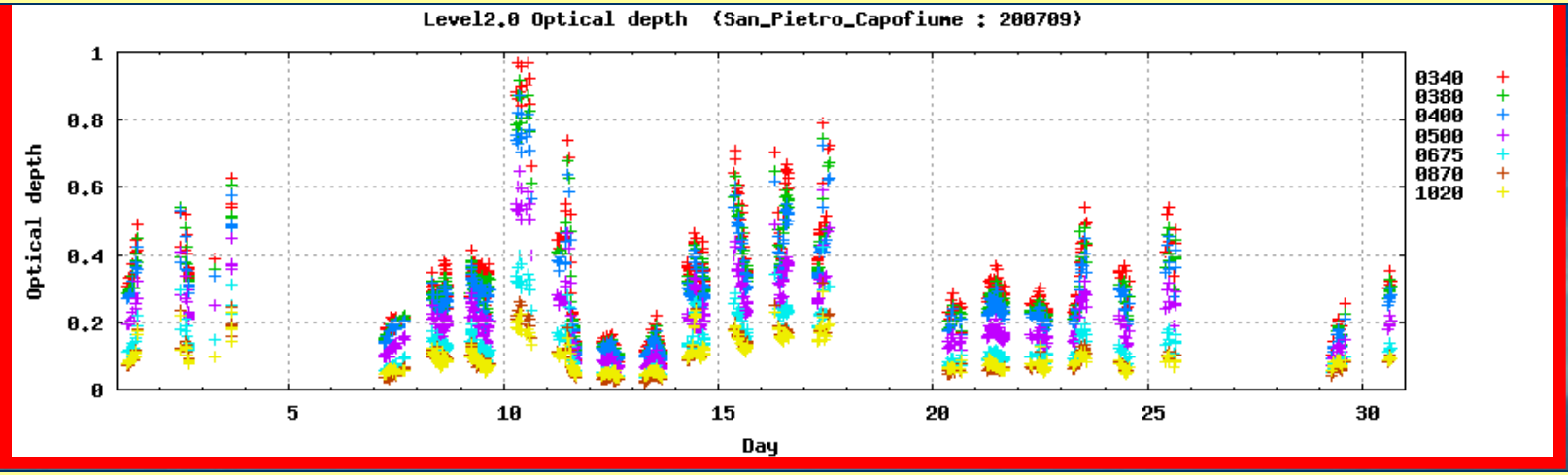

SSA = columnar aerosol single scattering albedo at the various wavelengths

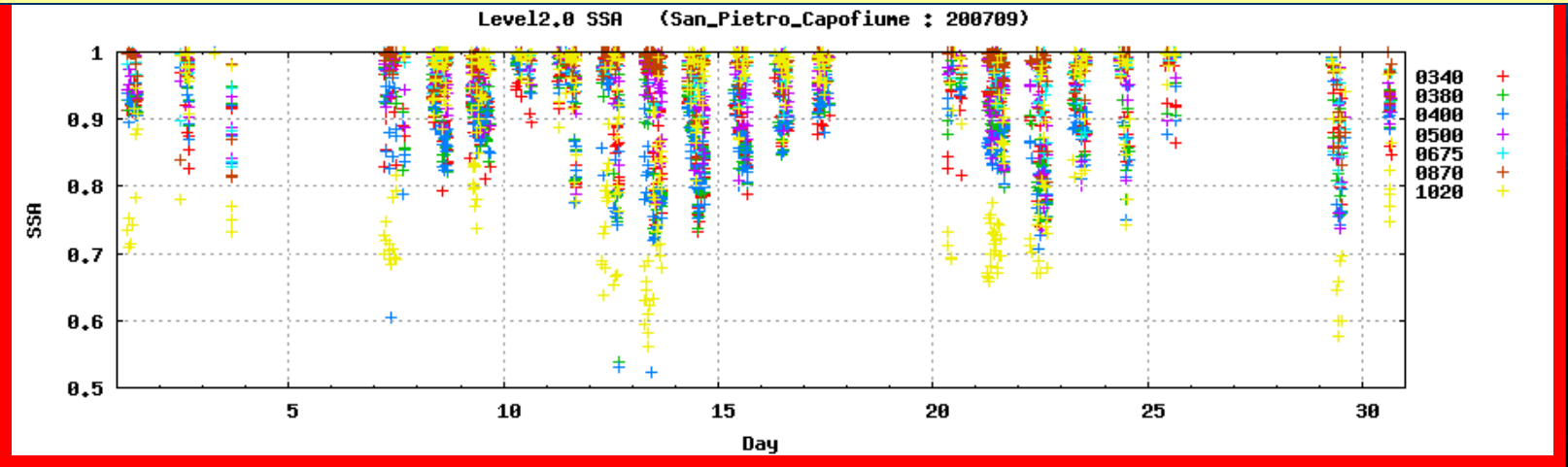

Comparison between the scatter plots of diurnally averaged values of DARF term ΔDF_{BoA} versus the daily mean values of $\tau_a(0.55\ \mu m)$ calculated for the 18 AERO-CLOUDS golden days using the VS1 (left) and VS4 (right) surface reflectance models. The different colours are used to mark the classes of exponent α, ranging between 0.0 and 2.0.

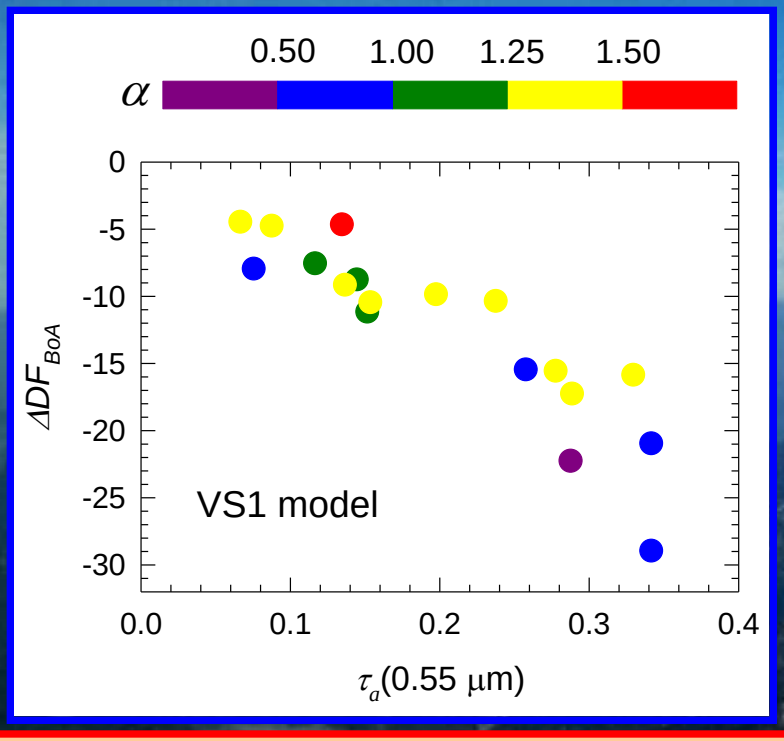

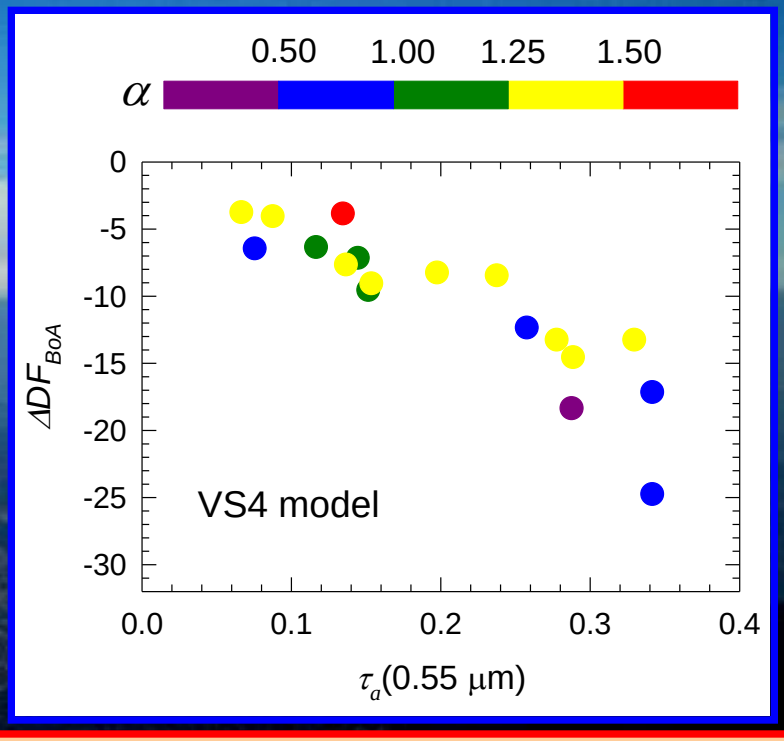

The comparison shows that ΔDF_{BoA} decreases almost linearly with $\tau_a(0.55\ \mu m)$, presenting a slightly more marked slope for the lower surface albedo of model VS1, and more limited variations as a function of α in the VS4 case.

Comparison between the scatter plots of the diurnally averaged values of DARF term ΔDF_{ToA} versus the daily average values of $\tau_a(0.55\ \mu m)$ calculated for the 18 AEROCLOUDS golden days using the VS1 (left) and VS4 (right) surface reflectance models. The different colours are used to mark the classes of exponent α., ranging between 0.0 and 2.0.

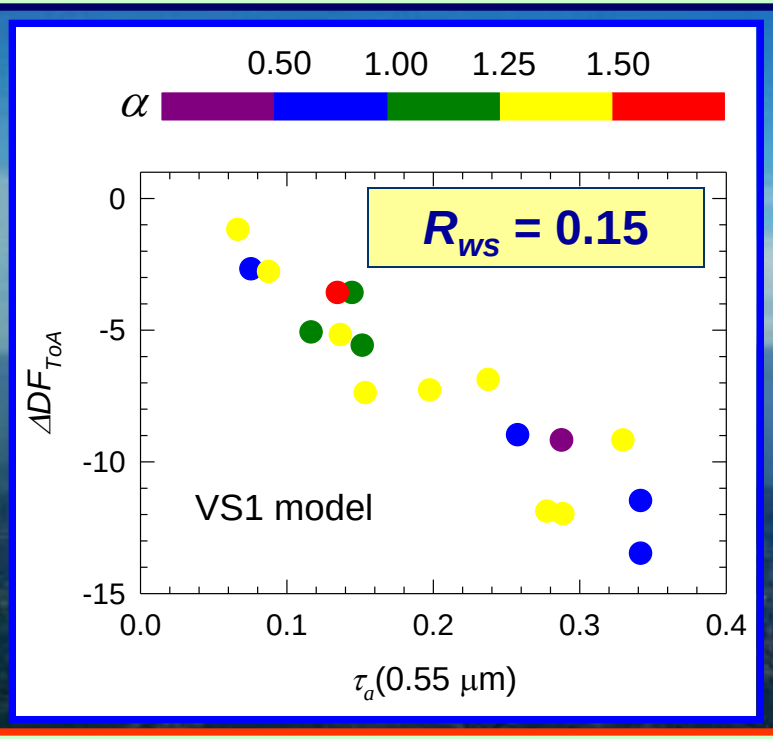

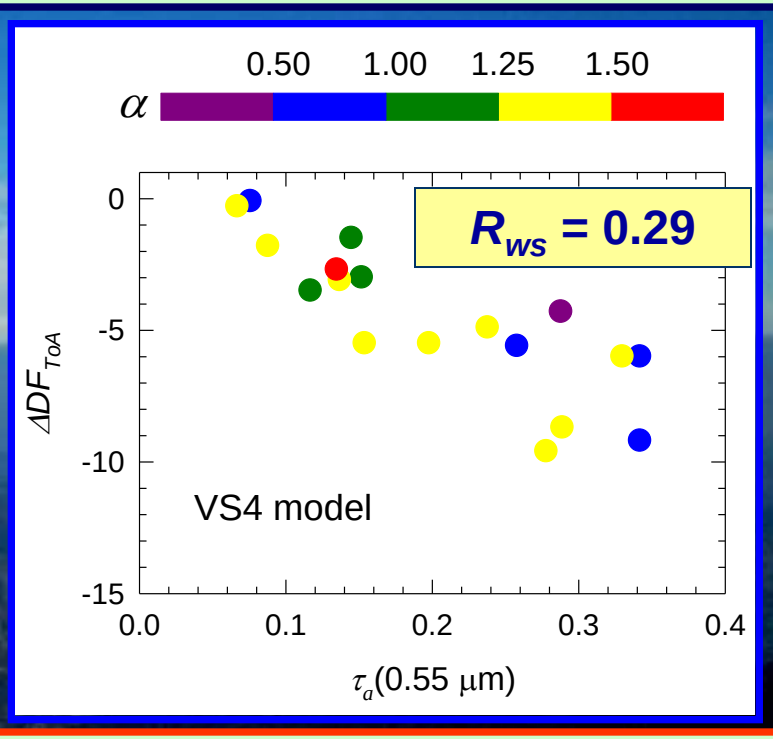

The comparison indicates that ΔDF_{ToA} decreases almost linearly with $\tau_a(0.55\ \mu m)$, presenting a more marked slope for the lower reflectance conditions of VS1 Model, the scatter of data being substantially due to the different size-distribution features and optical properties of columnar aerosol.

Comparison between the scatter plots of diurnally averaged values of DARF term ΔDF_{Atm} versus the daily mean values of $\tau_a(0.55\ \mu m)$ calculated for the 18 AERO-CLOUDS golden days using the VS1 (left) and VS4 (right) surface reflectance models. The different colours are used to mark the classes of exponent α., ranging between 0.0 and 2.0.

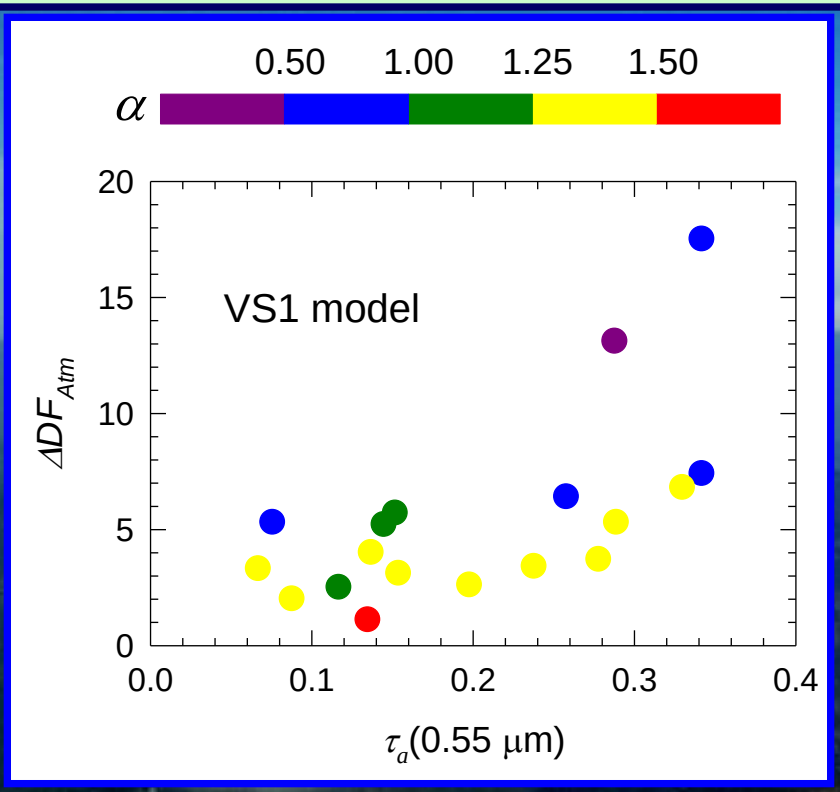

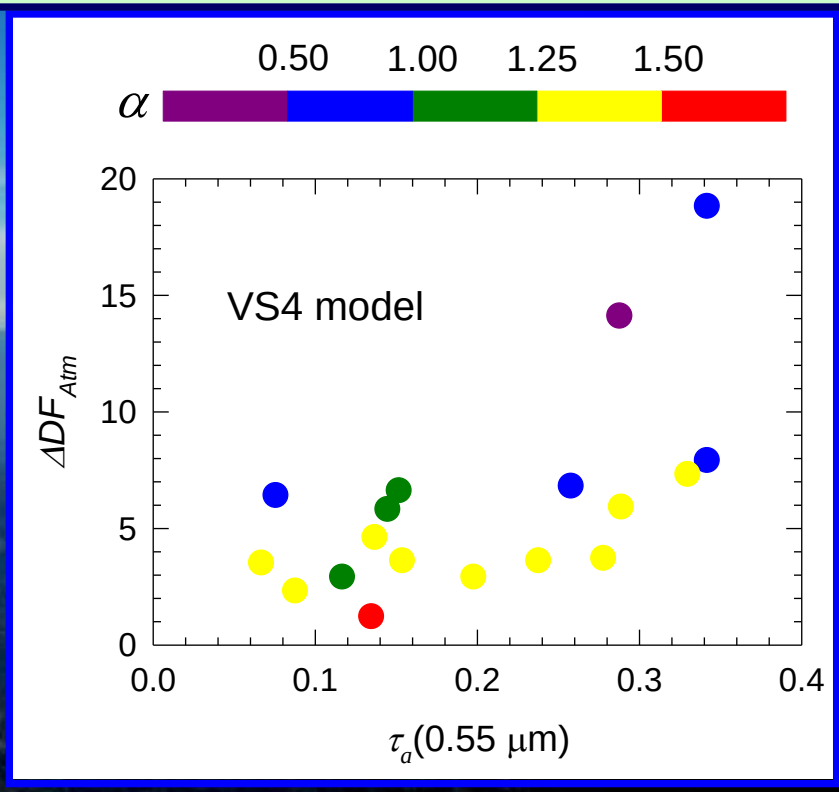

The comparison shows that ΔDF_{Atm} causes an atmospheric warming effect clearly Increasing with $\tau_a(0.55\ \mu m)$, presenting very similar variations in the two cases.

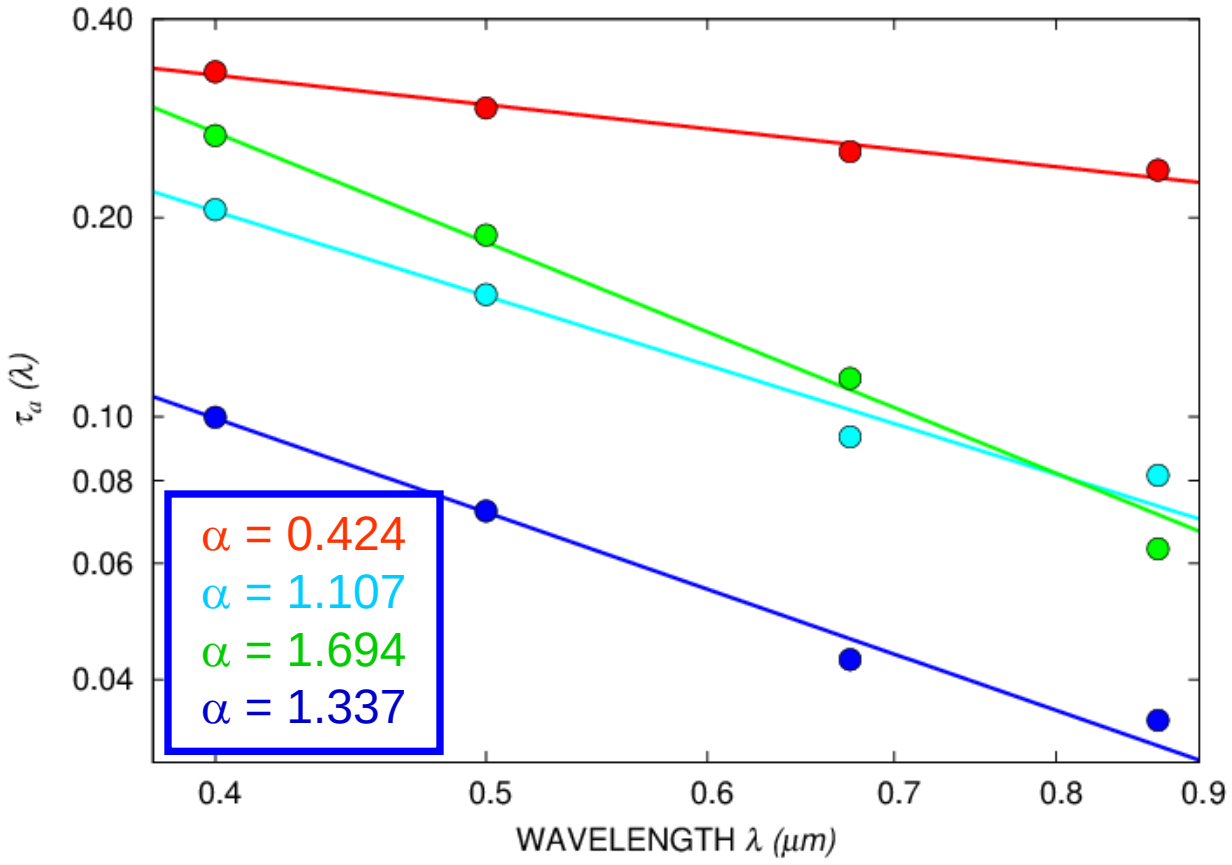

Examples of Ångström (1964) best-fit procedure applied to spectral series of aerosol optical thickness $\tau_a(\lambda)$ measured at SPC over the 0.40-0.87 μm wavelength range, on four AERO-CLOUDS golden days characterized by different columnar aerosol loads, for:

(i) continental aerosol mixed with Saharan dust (July 17, 2007) (red circles);
(ii) continental aerosol from the Arctic and North Europe areas (October 15, 2007) (cyan circles);
(iii) continental aerosol from Eastern Europe (December 19, 2007) (green circles); and
(iv) mixed marine and continental aerosol from North Atlantic Ocean and Western Europe areas (March 13, 2008) (blue circles).

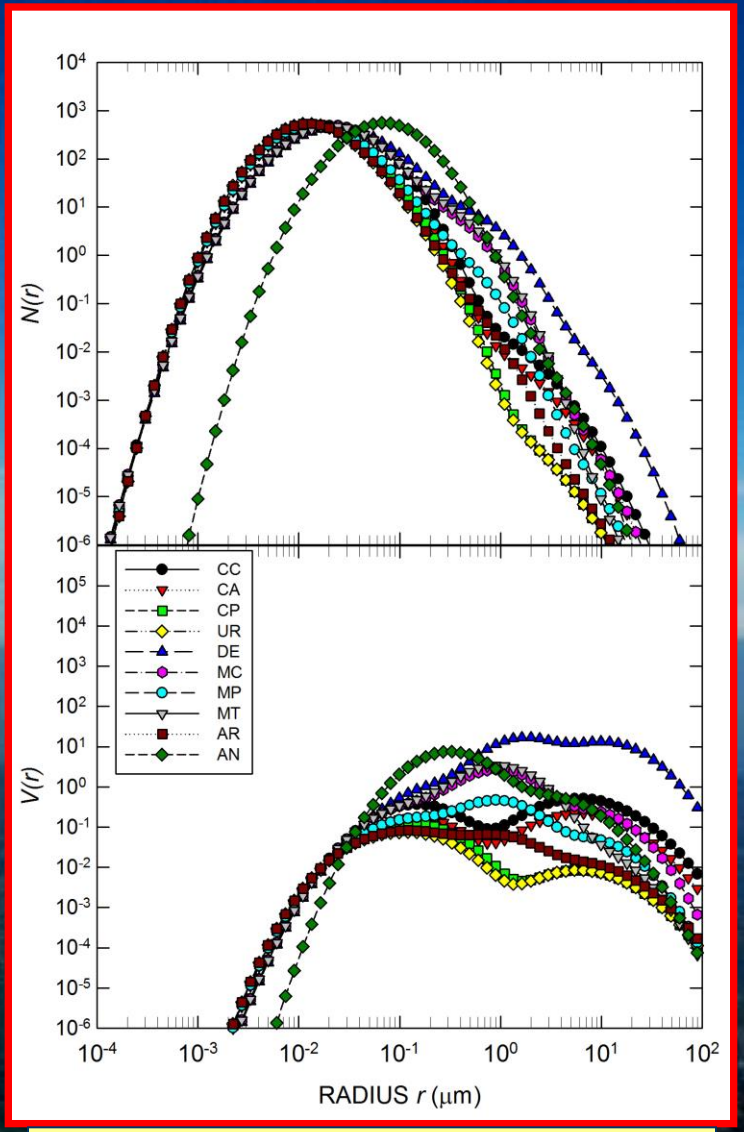

10 OPAC aerosol models (Hess et al., 1998)

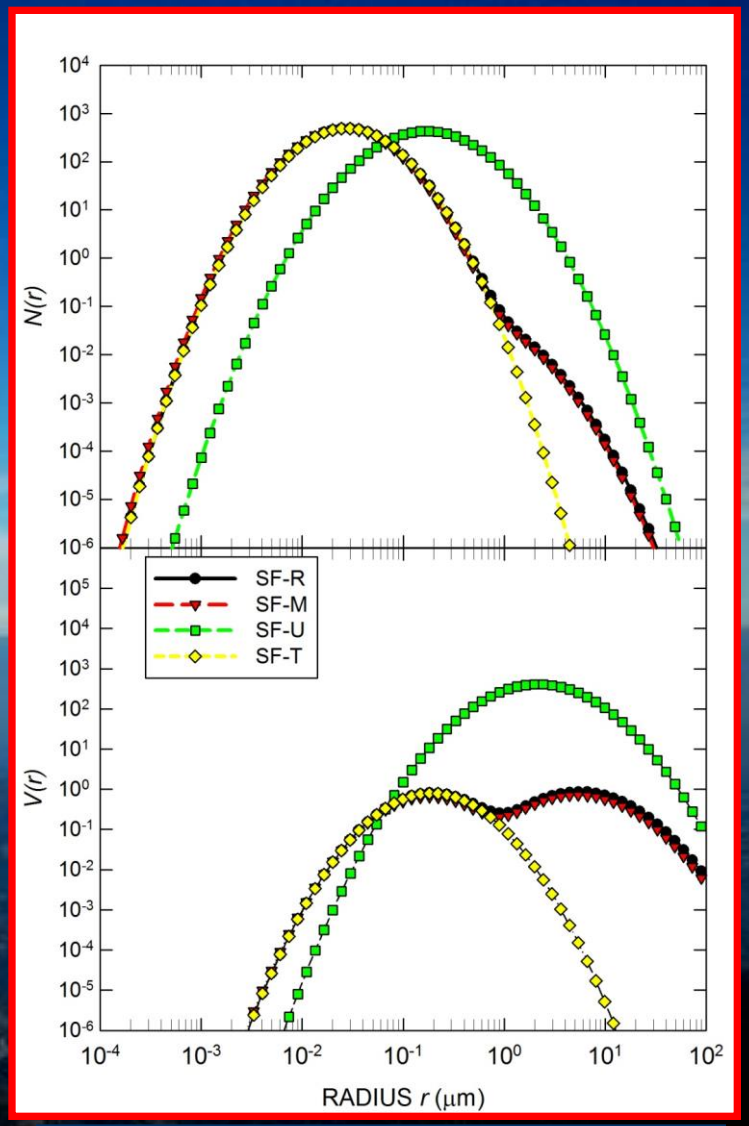

Aerosol models of Shettle and Fenn (1977)

OPAC = Optical Properties of Aerosols and Clouds

R = Rural; M = Maritime; U = Urban; T = Tropospheric (background).

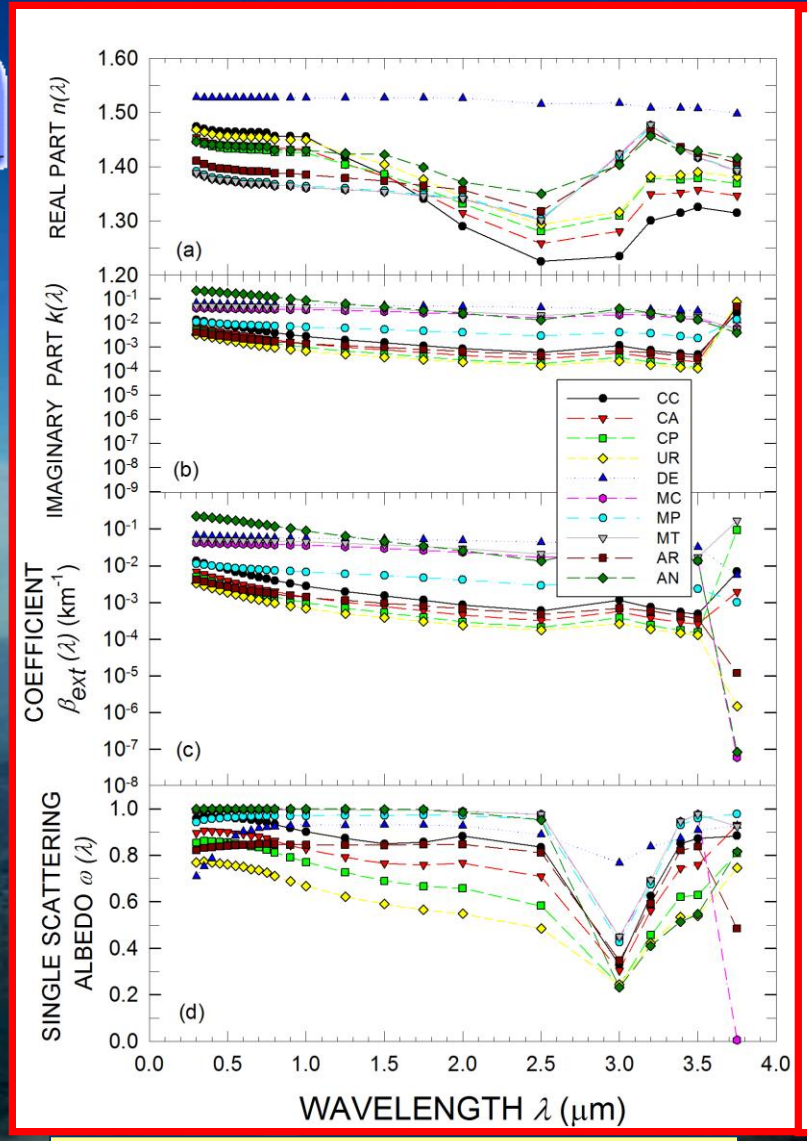

10 OPAC aerosol models of (Hess et al., 1998)

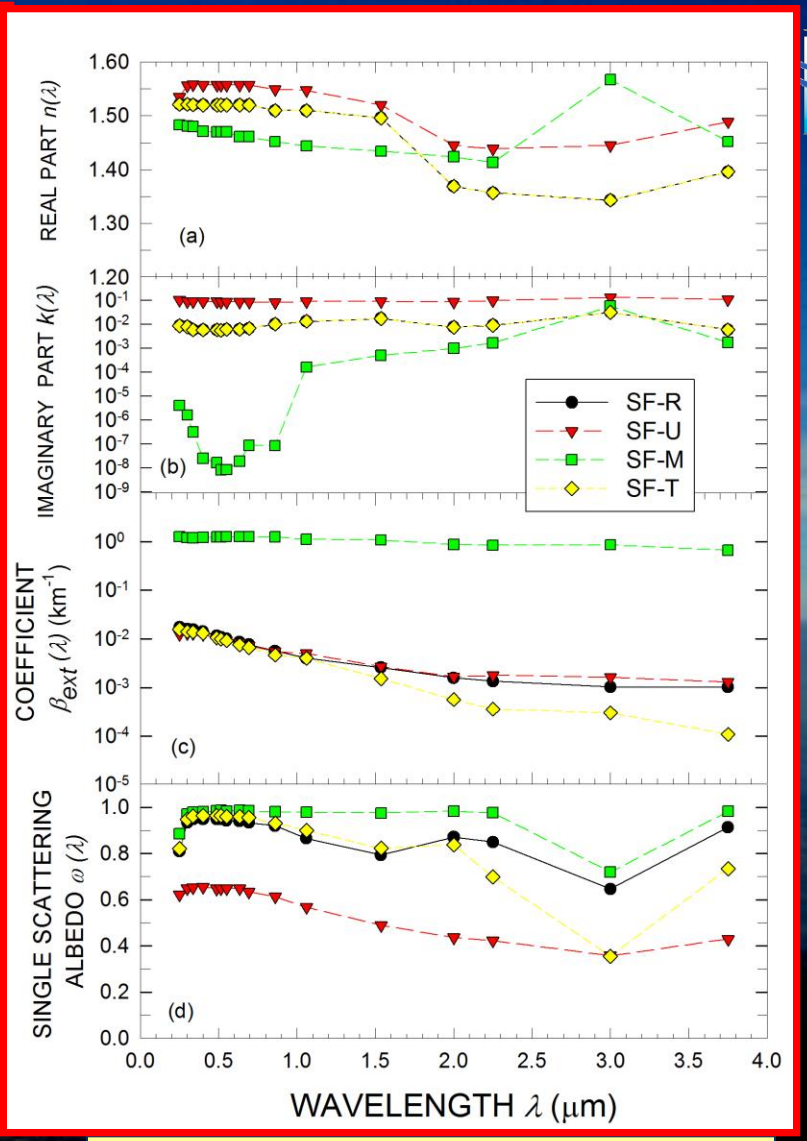

Aerosol models of Shettle and Fenn (1977)

The instantaneous DARF terms $\Delta F(t)_{ToA}$ and $\Delta F(t)_{BoA}$ vary as a function of solar zenith angle θ_o during the sunlit period, and depend closely on the following parameters:

(1) **aerosol optical thickness** $\tau_a(\lambda)$,

(2) **columnar aerosol radiative parameters,** and

(3) **surface reflectance** characteristics.

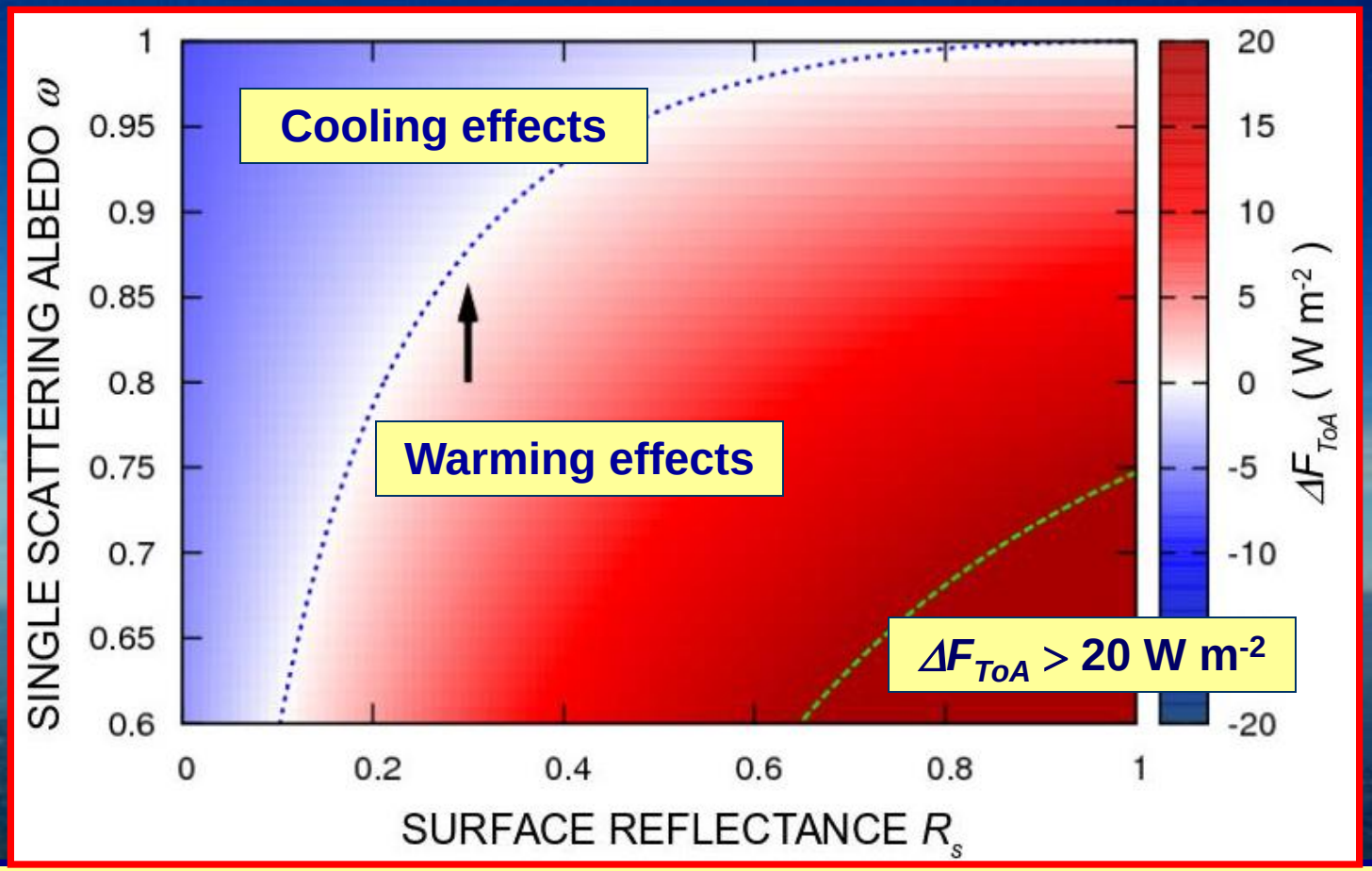

Three-dimensional representation of the change ΔF_{ToA} (W m^{-2}) caused by columnar aerosol in the upwelling flux of short-wave radiation at the ToA-level of the atmosphere as a function of columnar aerosol single scattering albedo ω and surface reflectance R_s, obtained for aerosol optical thickness τ_a = 0.10, and atmospheric transmittance equal to 0.75.

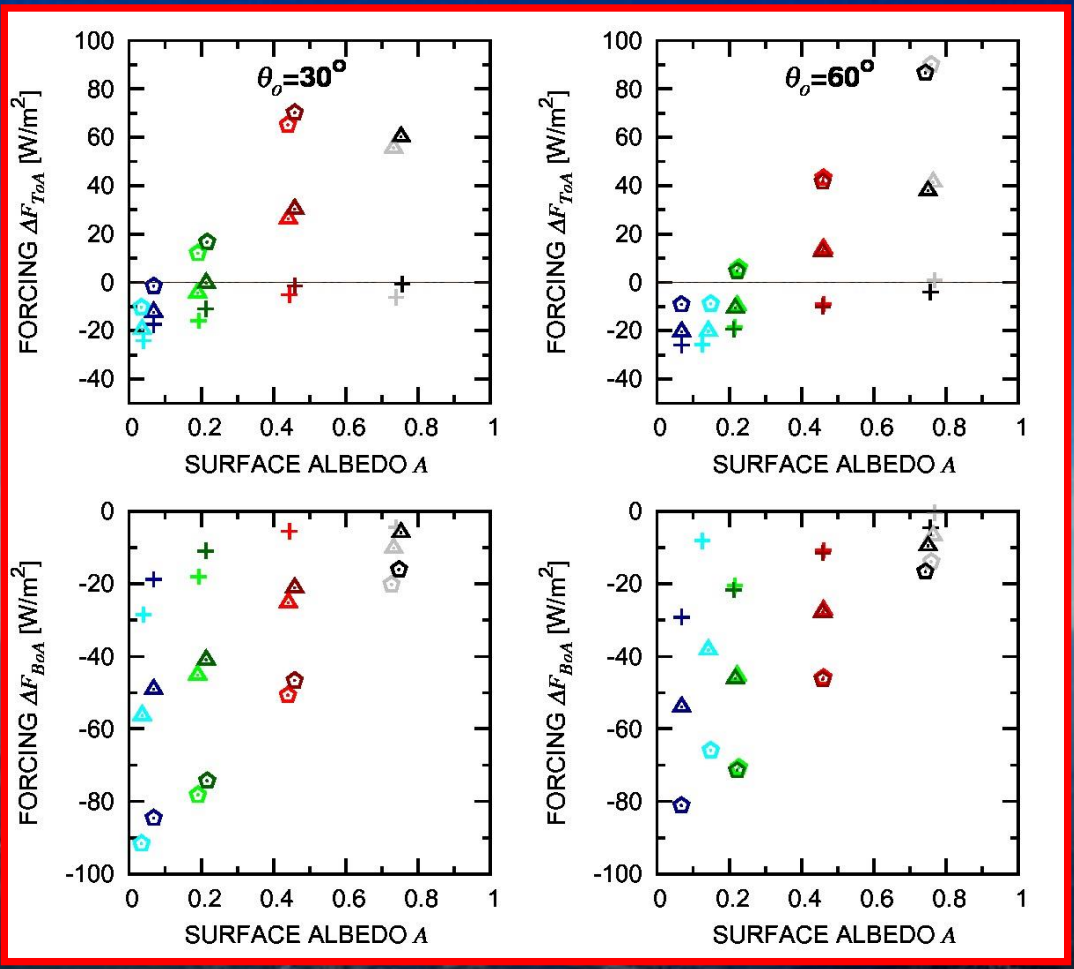

Instantaneous DARF terms ΔF_{ToA} (upper part) and ΔF_{BoA} (lower part) plotted as a function of broadband surface albedo $A(\theta_o)$, for aerosol optical depth $\tau_a(0.55\ \mu m)$ = 0.30 and solar zenith angles θ_o = 30° (left) and θ_o = 60° (right), as calculated for the four Shettle and Fenn (1977) aerosol models SF-M, SF-R, SF-T and SF-U, and for the BRDF non-Lambertian (light colours) and the equivalent isotropic Lambertian (dark colours) surface reflectance models OS1 (blue), VS1 (green), BS1 (red) and PS1 (gray).

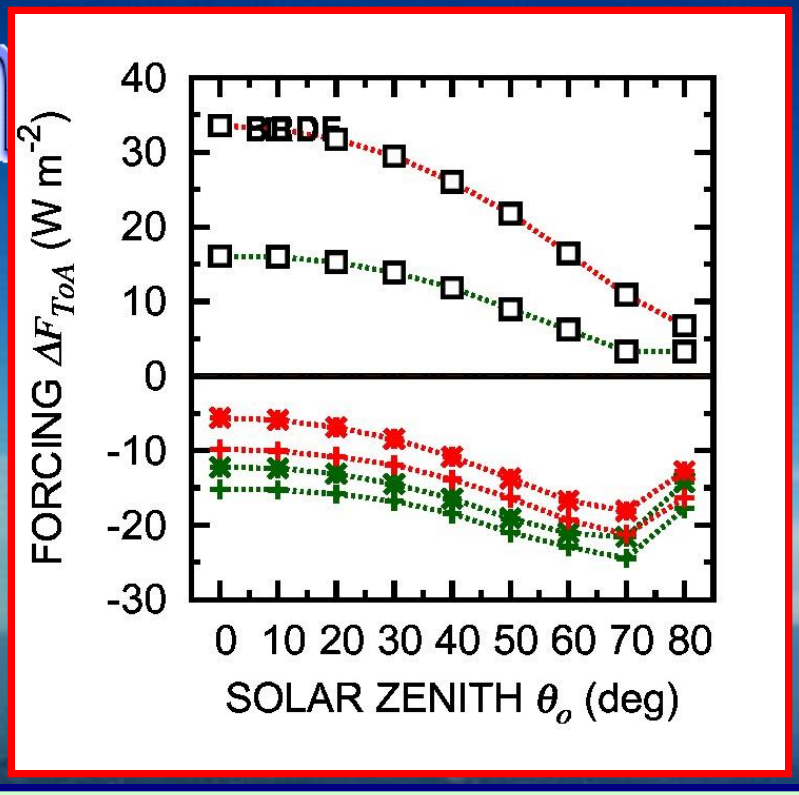

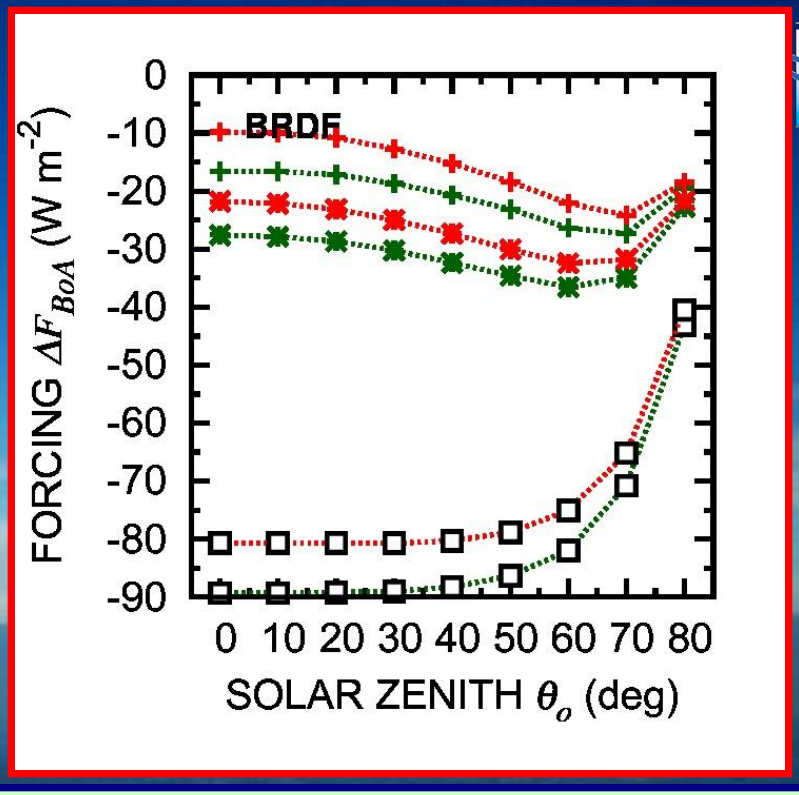

Instantaneous direct aerosol-induced radiative forcing terms ΔF_{ToA} (left) and ΔF_{BoA} (right) calculated for $\tau_a(0.55\ \mu m)$ = 0.30, and nine selected values of solar zenith angle θ_o (taken in steps of 10° from 0° to 80°), calculated for the four Shettle and Fenn (1979) aerosol models, and (ii) the VS1 (green), and BS1 (red) models represented for BRDF non-Lambertian surface reflectance characteristics.
Open symbols give the absolute differences between Lambertian and non-Lambertian evaluations of the DARF terms.

Lidar measurements were also performed during the AERO-CLOUDS experiment using the ISAC-CNR/ENEA lidar system,

Vertical profiles of backscattering ratio at 532 nm wavelength (azure curve) and depolarization degree (fuchsia curve) measured at SPC on March 18, 2009 (11:00 GMT).

Ground-level volume backscattering ratio derived from the nephelometer and PSAP data recorded at SPC on March 18, 2009 (11:00 GMT).

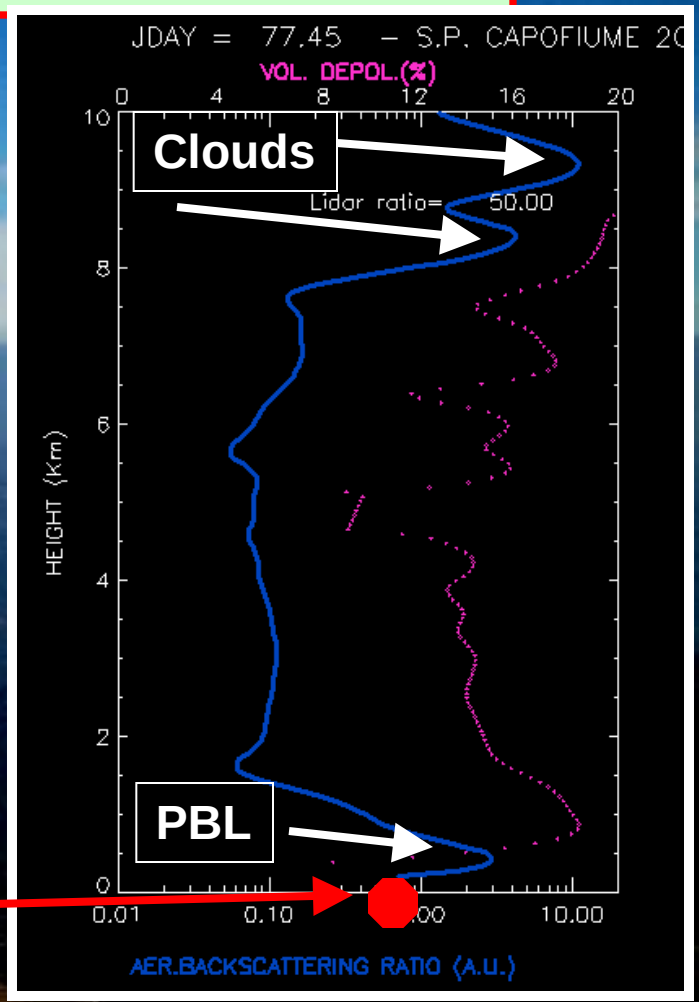

Regular measurements of the volume scattering coefficient $\beta_{sca}(530\ nm)$ (m^{-1}) and volume absorption coefficient $\beta_{abs}(573\ nm)$ (m^{-1}) were performed at SPC using the M903 Radiance Research nephelometer (*left*) and the Particle Soot Absorption Photometer (PSAP) of the Radiance Research (right).

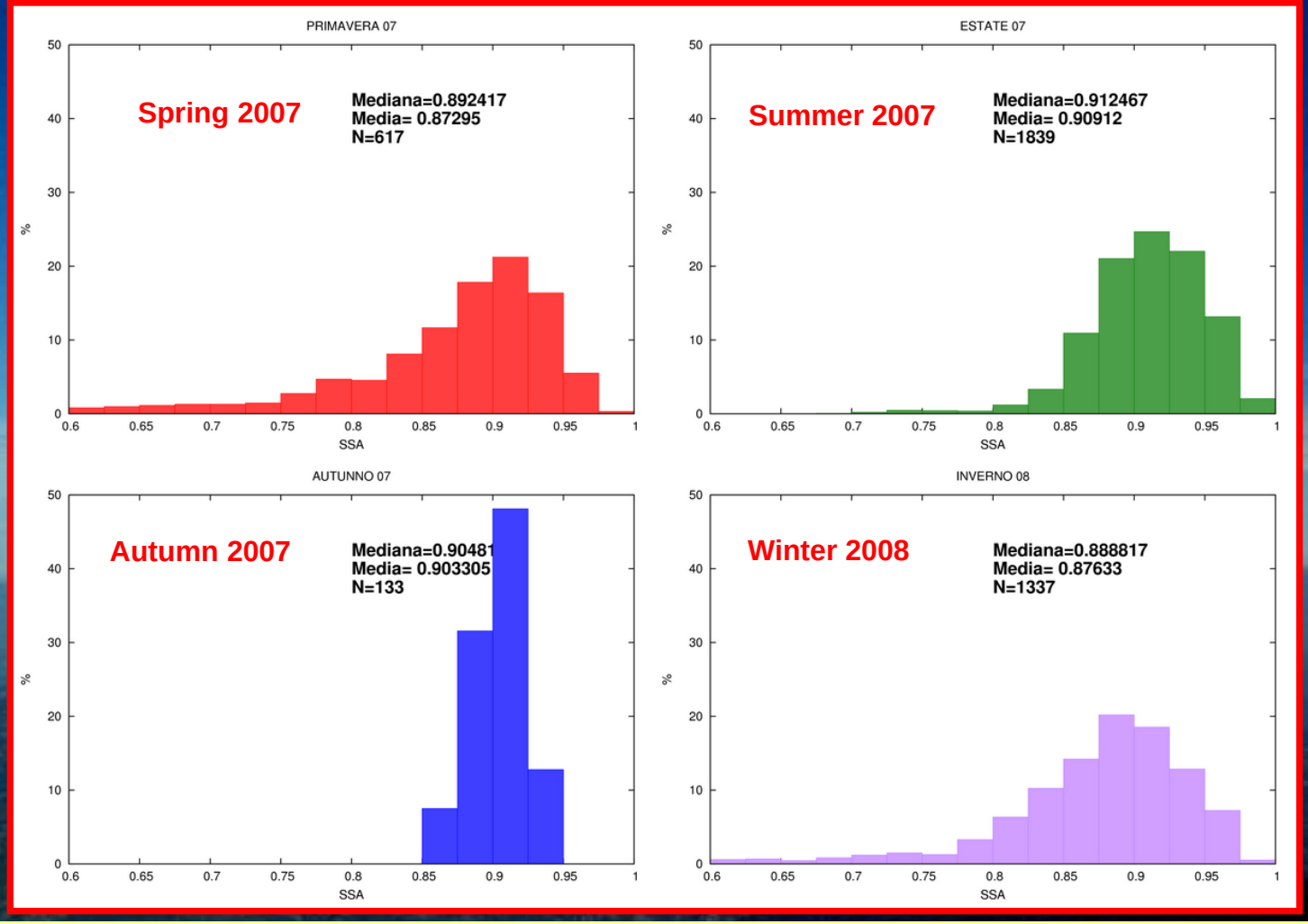

Seasonal relative frequency histograms of the ground-level aerosol single scattering albedo $\omega_o(550\ nm)$ measured at SPC from May 2007 to March 2008. Median values are equal to 0.89 in spring 2007, 0.91 in summer 2007, 0.90 in autumn 2007 and 0.89 in winter 2008.

Views of the aerosol sampling San Pietro Capofiume (SPC) station

Aerosol sampling measurements were regularly performed during the AEROCLOUDS experiment at the SPC station, using:

(1) HR-Tof (high-resolution time-of-flight) Aerosol Mass Spectrometers (AMS) to study the on-line evolution of the main chemical components ($SO_4^{=}$, NO_3^{-}, NH_4^{+} and organics) of atmos-pheric aerosol in relation to real-time changes in meteorological and photochemical conditions, local or long-range transport events,

(2) five-stage Berner impactors (LPI 80/0.05) with 50% size cut at 0.05, 0.14, 0.42, 1.2, 3.5 and 10 μm aero-dynamic diameter to carry out aerosol samplings and obtain a full characterization of the whole aerosol mass collected as a function of particle size (water soluble organic carbon (WSOC), water insoluble carbon (WINC) and water soluble inorganic aerosol components (NH_4^{+}, Na^{+}, K^{+}, Ca_2^{+}, Mg_2^{+}, Cl^{-}, NO_3^{-}, $SO_4^{=}$), and

(3) Differential Mobility Particle Sizer (DMPS), for measuring the aerosol concentration and size distribution of particles with optical diameter between 3 and 600 nm.

DEFINITIONS:

The instantaneous DARF term $\Delta F(t)_{ToA}$ (at the ToA-level) induced at a certain time *t* of the day by aerosol particles suspended in a clear-sky atmosphere can be represented in terms of the following formula:

$$\Delta F(t)_{ToA} = F(t)_{net} - F(t)_{net^*} , \quad (1)$$

where (**a**) the ToA-level net flux $F(t)_{net}$ is given by the difference between the short-wave downwelling flux $F\downarrow(t)$ and the short-wave upwelling flux $F\uparrow(t)$, both determined at the ToA-level for an atmosphere including all its constituents, i.e.:

$$F(t)_{net} = F\downarrow(t) - F\uparrow(t) , \quad (2)$$

where the downwelling flux $F\downarrow(t)$ is obviously independent of the aerosol extinction processes taking place in the atmosphere, and (**b**) the net flux $F(t)_{net^*}$ at ToA-level is given by the difference between the corresponding short-wave downwelling flux $F\downarrow(t)^*$and short-wave upwelling flux $F\uparrow(t)^*$, both calculated in the pristine atmosphere without aerosols, i.e.:

$$F(t)_{net^*} = F\downarrow(t)^* - F\uparrow(t)^* , \quad (3)$$

where the downwelling flux $F\downarrow(t)^*$ is not altered by atmospheric aerosols. Therefore, flux $F\downarrow(t)^*$ in Eq. (3) is equal to flux $F\downarrow(t)$ given in Eq. (2).

Thus, the instantaneous term ΔF_{ToA} calculated from Eqs. (1), (2) and (3) is directly given by the difference,

$$\Delta F(t)_{ToA} = F\uparrow(t)^* - F\uparrow(t) , \quad (4)$$

which shows that this DARF term can be correctly evaluated by simply subtracting the upward solar radiation flux emerging from the real atmosphere with aerosols from the upwelling solar radiation flux emerging from the pristine atmosphere without aerosols.

The instantaneous aerosol radiative forcing $\Delta F(t)_{BoA}$ at the surface (i.e. at the BoA-level) gives a measure of the aerosol-induced perturbation in the net flux reaching the surface.

Therefore, $\Delta F(t)_{BoA}$ can be defined as the difference between the net flux at surface-level in the atmosphere with aerosols and the net flux at the surface-level in the same atmosphere assumed without aerosols (Satheesh and Ramanathan, 2000; Bush and Valero, 2002, 2003).

It can be expressed at a given time as the difference:

$$\Delta F(t)_{BoA} = \Phi(t)_{net} - \Phi(t)_{net^*} , \qquad (5)$$

where, the net flux $\Phi(t)_{net}$ at the surface is given by the difference between the downwelling flux $\Phi\downarrow(t)$ and the upwelling flux $\Phi\uparrow(t)$, i.e.

$$\Phi(t)_{net} = \Phi\downarrow(t) - \Phi\uparrow(t). \qquad (6)$$

The instantaneous aerosol radiative forcing $\Delta F(t)_{BoA}$ at the surface (i.e. at the BoA-level) gives a measure of the aerosol-induced perturbation in the net flux reaching the surface.

Therefore, $\Delta F(t)_{BoA}$ can be defined as the difference between the net flux at surface-level in the atmosphere with aerosols and the net flux at the surface-level in the same atmosphere assumed without aerosols (Satheesh and Ramanathan, 2000; Bush and Valero, 2002, 2003).

It can be expressed at a given time as the difference:

$$\Delta F(t)_{BoA} = \Phi(t)_{net} - \Phi(t)_{net^*} , \qquad (5)$$

where, the net flux $\Phi(t)_{net}$ at the surface is given by the difference between the downwelling flux $\Phi\downarrow(t)$ and the upwelling flux $\Phi\uparrow(t)$, i.e.

$$\Phi(t)_{net} = \Phi\downarrow(t) - \Phi\uparrow(t). \qquad (6)$$

The diurnally averaged DARF terms at ToA-level, BoA-level and within the atmosphere (Atm) are roughly proportional to the aerosol optical depth, and vary appreciably as a function of the microphysical and optical parameters of columnar aerosol. Therefore, a triplet of DARF parameters not depending on AOD are usually considered, known as "aerosol forcing efficiencies" E_{ToA}, E_{BoA} and E_{Atm}. The first two parameters are obtained by dividing the values of ΔDF_{ToA} and ΔDF_{BoA} by the daily mean value of $\tau_a(0.55\ \mu m)$, or alternatively by the daily averaged value of $\tau_a(\lambda)$ over the 0.30 – 0.70 μm broadband spectral range (as done in the TARFOX experiment, by Hignett et al. (1999) and Russell et al. (1999). Efficiency E_{Atm} is more simply assumed to be equal to the difference EToA – *EBoA.*

Comparison between the scatter plots of the diurnally averaged values of ΔDF_{ToA} versus the daily mean values of $\tau_a(0.55\ \mu m)$ calculated for the 18 AEROCLOUDS Golden days using the VS1 (left) and VS4 (right) surface reflectance models, for different classes of columnar aerosol single scattering albedo ω_o.

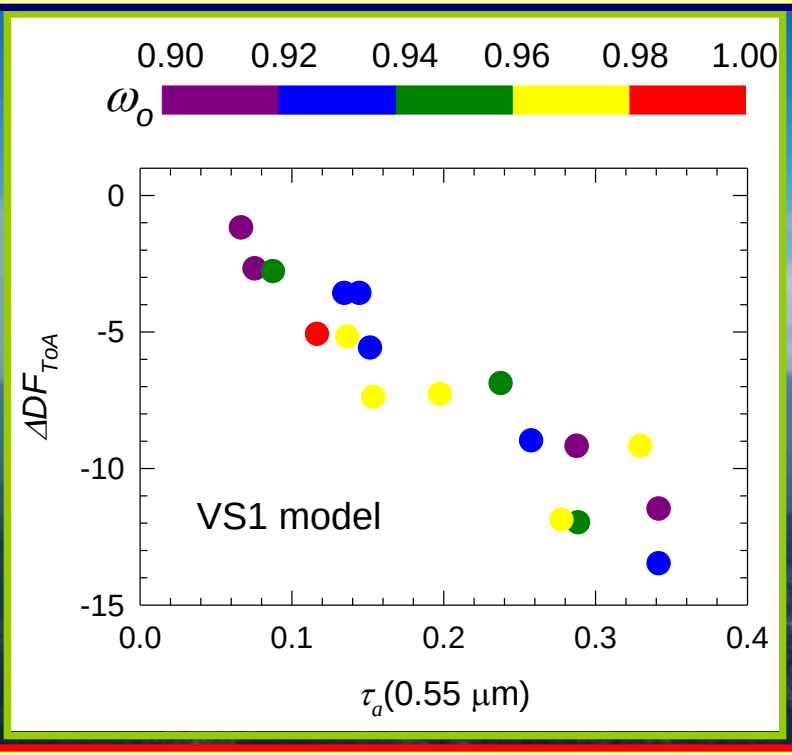

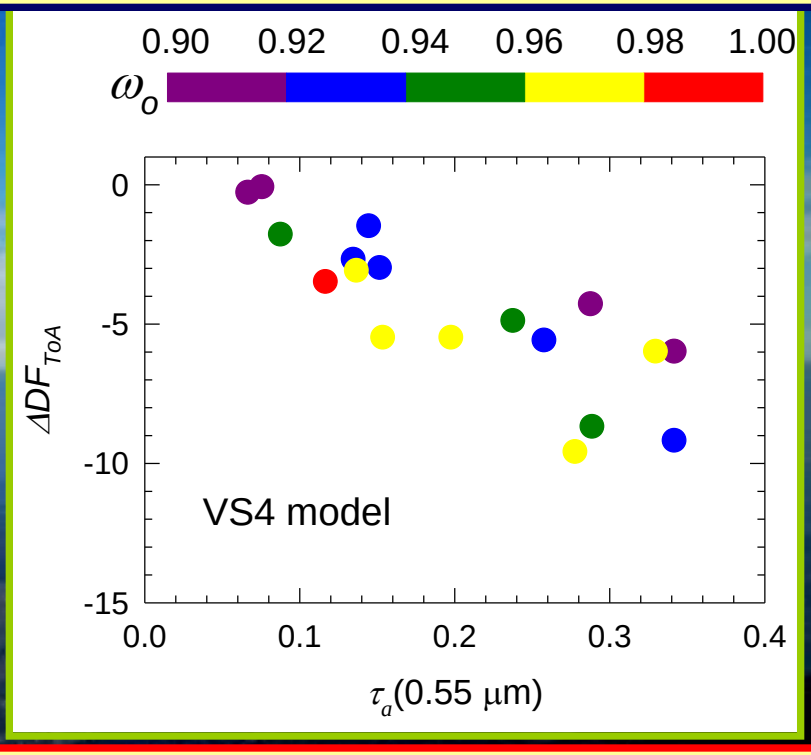

The comparison shows that ΔDF_{ToA} decreases almost linearly with $\tau_a(0.55\ \mu m)$, presenting an average slope, which is evidently more marked for the lower VS1 surface reflectance characteristics, and an appreciably wider scatter for the VS4 surface reflectance model.

Comparison between the scatter plots of diurnally averaged values of ΔDF_{BoA} versus the daily mean values of $\tau_a(0.55\ \mu m)$ calculated for the 18 AEROCLOUDS golden days using the VS1 (left) and VS4 (right) surface reflectance models for various classes of columnar aerosol single scattering ω_o.

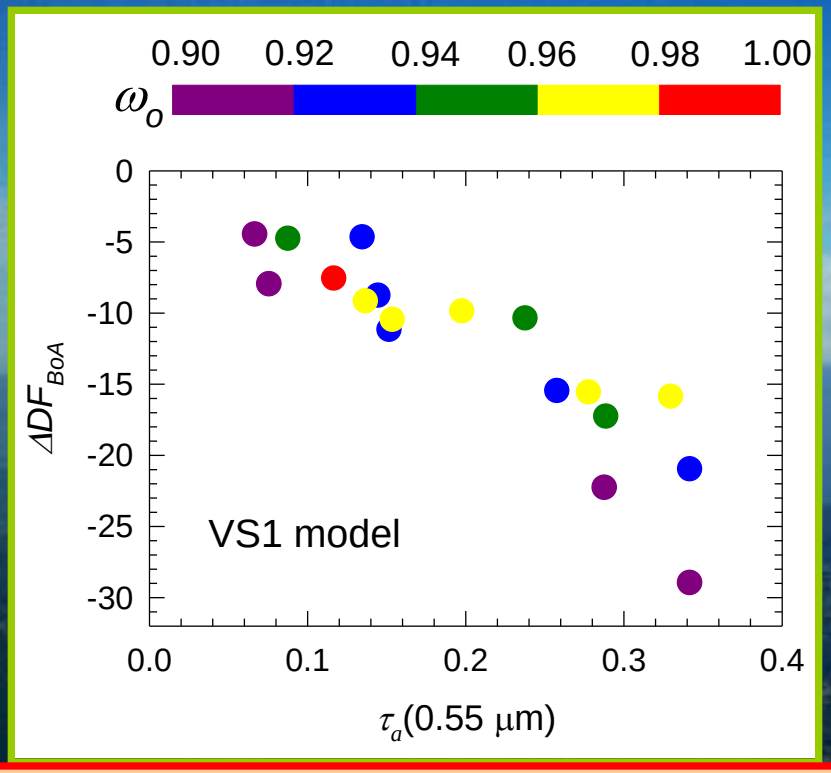

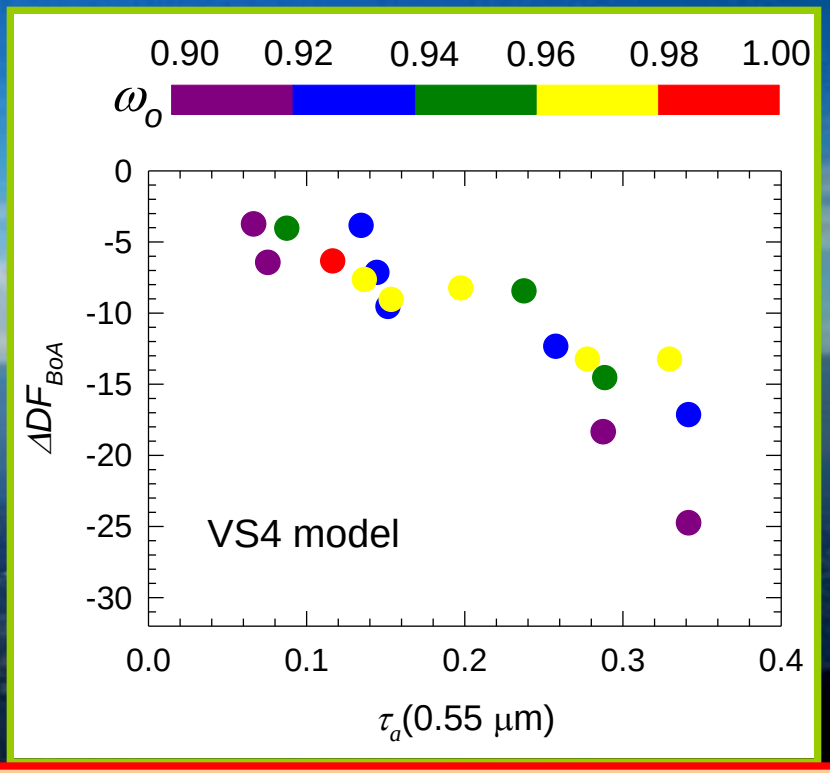

The comparison shows that ΔDF_{BoA} decreases almost linearly with $\tau_a(0.55\ \mu m)$, presenting a more marked average slope for the VS1 surface reflectance model and a slightly less pronounced slope for the higher reflectance features of model VS4.

Comparison between the scatter plots of diurnally averaged values of ΔDF_{Atm} versus the daily mean values of $\tau_a(0.55\ \mu m)$ calculated for the 18 AEROCLOUDS golden days using the VS1 (left) and VS4 (right) surface reflectance models and for the various classes of columnar aerosol single scattering albedo ω_o.

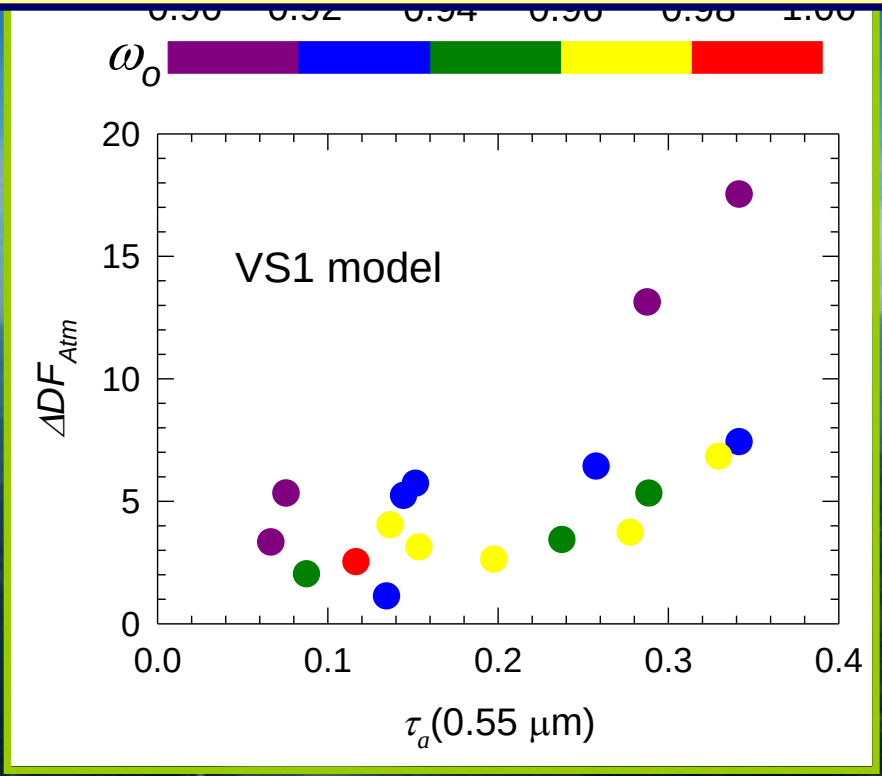

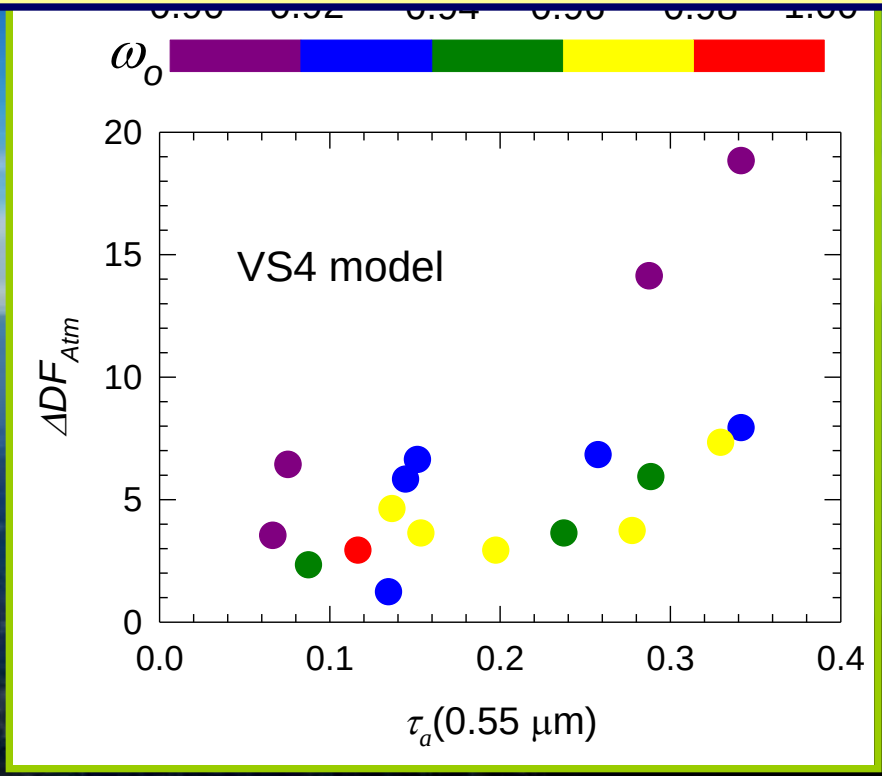

The comparison indicates that ΔDF_{Atm} increases with $\tau_a(0.55\ \mu m)$, presenting very similar changes in the VS1 and VS4 cases, providing evidence that the atmospheric warming due solar radiation absorption by aerosols depends only negligibly on the surface reflectance characteristics and the changes in ω_o.

Workshop on “Remote sensing of atmospheric aerosol, clouds, and aerosol-cloud interactions“, Bremen, December 16 – 19, 2013

Workshop on “Remote sensing of atmospheric aerosol, clouds, and aerosol-cloud interactions“, Bremen, December 16 – 19, 2013

Workshop on “Remote sensing of atmospheric aerosol, clouds, and aerosol-cloud interactions“, Bremen, December 16 – 19, 2013